Eionet Report - ETC/ATNI 2020/11

European air quality interim mapping under ETC/ATNI

Evaluation of AQ mapping using UTD measurement and CAMS forecast modelling data: an approach for more timely European AQ annual maps?

June 2021 version 2

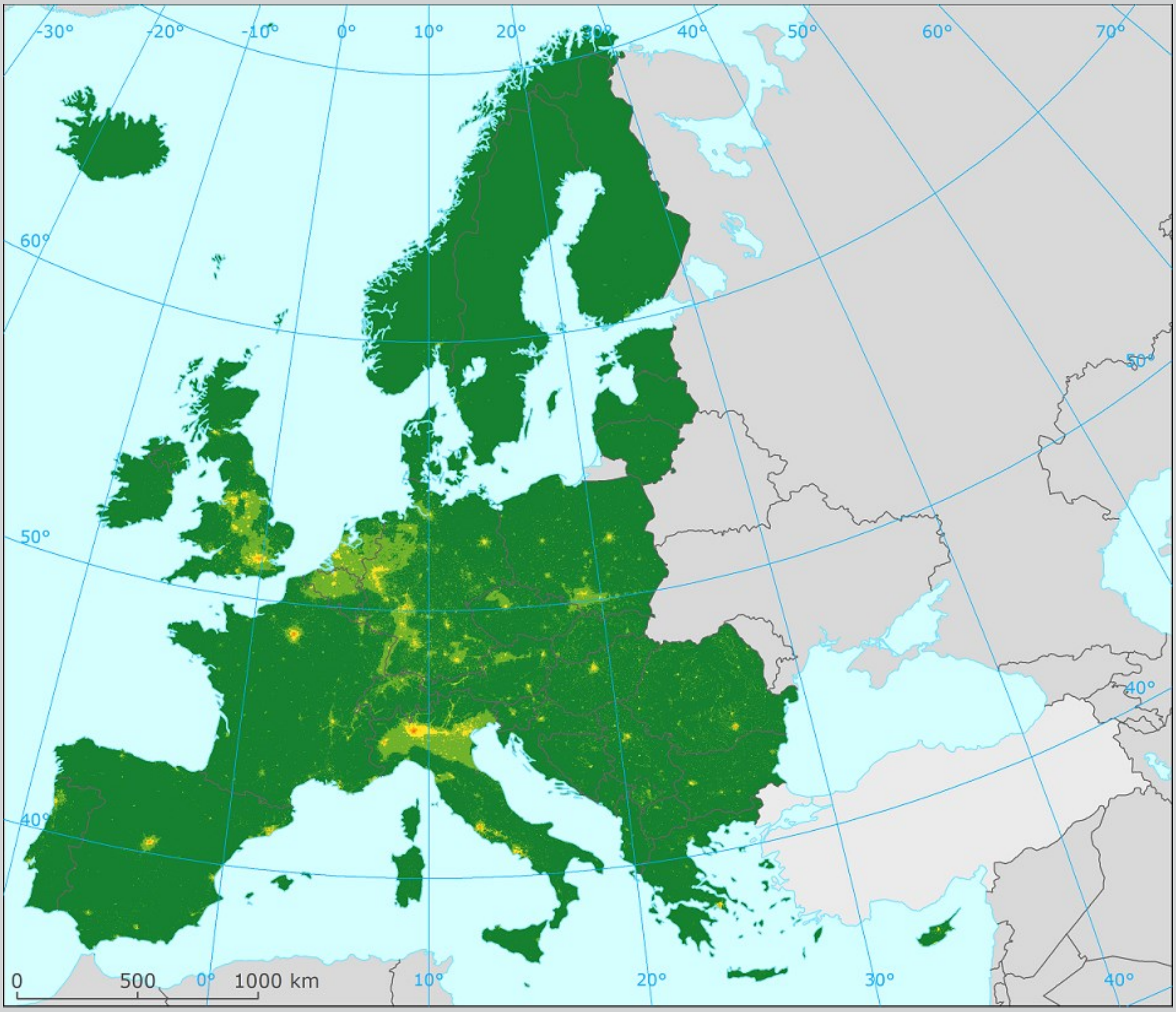

Authors:
Jan Horálek (CHMI), Paul Hamer (NILU), Markéta Schreiberová (CHMI), Philipp Schneider (NILU)

ETC/ATNI consortium partners:
NILU – Norwegian Institute for Air Research, Aether Limited, Czech Hydrometeorological Institute (CHMI), EMISIA SA, Institut National de l'Environnement Industriel et des risques (INERIS), Universitat Autònoma de Barcelona (UAB), Umweltbundesamt GmbH (UBA-V), 4sfera Innova, Transport & Mobility Leuven NV (TML)

European Environment Agency
European Topic Centre on Air pollution, transport, noise and industrial pollution

Cover picture: Interim concentration map of NO_2 annual average, 2019. Units: $\mu g \cdot m^{-3}$. (Map 5.2 of this report.)

The withdrawal of the United Kingdom from the European Union did not affect the production of the report.
Data reported by the United Kingdom are included in all analyses and assessments contained herein, unless otherwise indicated.

Author(s)
Jan Horálek, Markéta Schreiberová: Czech Hydrometeorological Institute (CHMI, Czechia)
Paul Hamer, Philipp Schneider: NILU - Norwegian Institute for Air Research (NILU, Norway)

ETC/ATNI c/o NILU
ISBN 978-82-93752-49-3

European Topic Centre on Air pollution, transport, noise and industrial pollution
c/o NILU – Norwegian Institute for Air Research
P.O. Box 100, NO-2027 Kjeller, Norway
Tel.: +47 63 89 80 00
Email: etc.atni@nilu.no
Web : https://www.eionet.europa.eu/etcs/etc-atni

Contents

Acknowledgements

The EEA task manager was Alberto González Ortiz.

Thanks are due to Jana Marková (CHMI, Czechia), who has prepared annual aggregations of the CAMS modelling data.

1 Introduction

Air quality European-wide annual maps based on spatial interpolation have been produced under ETC/ATNI (resp. previous consortia ETC/ACM and ETC/ACC) since 2005 (Horálek, 2021b and references therein). The mapping methodology combines monitoring data, chemical transport model results and other supplementary data using a linear regression model followed by kriging of the residuals produced from that model ('residual kriging'). Separate mapping layers (rural, urban background and urban traffic, where relevant) are created separately and subsequently merged together into the final map. In order to reflect the three steps applied, the methodology is called *Regression – Interpolation – Merging Mapping (RIMM)*. These maps have historically been constructed each year for the main air pollutants (PM_{10}, $PM_{2.5}$, O_3, NO_2), based on validated air quality (AQ) measurement data that are reported to EEA by its member and cooperating countries (and other voluntary reporting countries) under the AQ Directives. In order to add more information on concentration levels in areas with no measurements, the EMEP atmospheric dispersion model has been used as a secondary source of information, together with other supplementary data like altitude, land cover and meteorological data. However, due to the delays in production and availability of the validated AQ measurement data and the EMEP model output, the RIMM AQ maps of a year Y have typically not been available until May of year Y+2.

Apart from the validated measurement data uploaded to the EEA's AQ e-reporting database, preliminary measurement up-to-date (UTD) data are available in this same database on an hourly basis for most of the reporting countries. The validated data are stored in the so-called E1a data set, while the UTD data are in the E2a data set of the AQ e-reporting database. The E2a data, while not fully validated, are available at an earlier point, typically a few hours after their measurement. The earlier availability of E2a data creates an opportunity to provide AQ spatial mapping at an earlier date. In this report, we therefore evaluate the use of the E2a data for their potential at preparing interim annual spatial maps that would be available at an earlier point in time.

Since the objective of this report is to evaluate the use of E2a data, which are available one year in advance of the E1a data, we have opted to use within the RIMM methodology a modelling data product that is available also in advance of the E1a data. The Copernicus Atmosphere Monitoring Service (CAMS) ensemble forecast (the median of nine regional atmospheric dispersion models) model product is an attractive option because the CAMS ensemble forecast is produced each day, and so an entire year of model forecast data is already available on December 31st of each year. By contrast the EMEP model results, which have previously been used regularly in the RIMM methodology, are only available in September in the following year. The CAMS ensemble forecast was evaluated in the RIMM methodology in Horálek et al. (2021a), and was found to have skills comparable to the EMEP model. Our intended approach therefore has potential to deliver more timely interim AQ mapping that still maintains an adequate level of skill at representing the true pollutant spatial patterns.

As described in Horálek et al. (2021a), data gaps of E2a were identified in several areas. In order to overcome this obstacle, it was suggested to estimate so-called pseudo stations data in the areas with the lack of E2a stations, based on the regression relation between E2a data from year Y and validated E1a data from year Y-1. In order to improve the estimates of the pseudo data, the ratio of the modelling results from years Y and Y-1 is also used in the regression relation.

In this report, we present and evaluate AQ interim mapping of the PM_{10} annual average, the NO_2 annual average and the ozone indicator SOMO35, based on E2a (UTD) measurement data and CAMS forecast model data. We also briefly check the possibility to prepare the interim map for $PM_{2.5}$, however low number of stations with the E2a data prevents us from such mapping. We examine the interim annual maps for 2017. We include an evaluation of the quality of the three produced maps comparing them with the validated E1a data, using the statistical indicators R^2, standard error, RMSE, relative RMSE, and bias. Next to this, we also present the interim maps for 2019, for the three pollutants PM_{10}, NO_2 and ozone. The evaluation of these maps using the validated E1a 2019 data has not been performed, as these data were not available in the time designated for this study. For the interim 2019 maps, we have performed only the cross-validation based on the E2a data.

Chapter 2 describes the methodological aspects. Chapter 3 documents input data and the evaluation approach. Chapter 4 presents the evaluation of the spatial mapping results for the preliminary maps for 2017. Chapter 5 presents the preliminary maps for 2019. Chapter 6 gives the conclusions and recommendations. Annex provides maps of measurement stations used for mapping and validation.

2 Mapping Methodology

2.1 Spatial Mapping Methodology

The mapping methodology used in the Regression – Interpolation – Merging Mapping method (RIMM) as routinely used in the spatial mapping under the ETC/ATNI (Horálek et. al., 2021b) consists of a linear regression model followed by kriging of the residuals from that regression model (residual kriging):

$$\hat{Z}(s_0) = c + a_1 X_1(s_0) + a_2 X_2(s_0) + \cdots + a_n X_n(s_0) + \hat{\eta}(s_0) \qquad (2.1)$$

where $\hat{Z}(s_0)$ is the estimated concentration at a point s_o,
$X_1(s_0)$ is the chemical transport model (CTM) data at point s_o,
$X_2(s_0),\ldots, X_n(s_0)$ are *n-1* other supplementary variables at point s_o,
$c, a_1, a_2,\ldots, a_n$ are the *n+1* parameters of the linear regression model calculated based on the data at the points of measurement,
$\hat{\eta}(s_0)$ is the spatial interpolation of the residuals of the linear regression model at point s_o, based on the residuals at the points of measurement.

For different pollutants and area types (rural, urban background, and for PM_{10} and NO_2 also urban traffic), different supplementary data are used. The spatial interpolation of the regression residuals is carried out using ordinary kriging, according to

$$\hat{\eta}(s_0) = \sum_{i=1}^{N} \lambda_i \eta(s_i) \qquad \text{with } \sum_{i=1}^{N} \lambda_i = 1, \qquad (2.2)$$

where $\hat{\eta}(s_0)$ is the interpolated value at a point s_o,
N is the number of the measurement points used in the interpolation, which is fixed based on the variogram; in any case, $20 \le N \le 50$,
$\eta(s_i)$ is the residual of the linear regression model at the measurement point s_i,
$\lambda_1,\ldots, \lambda_N$ are the estimated weights based on the variogram, see Cressie (1993).

For PM_{10}, prior to linear regression and interpolation, a logarithmic transformation to measurements and CTM modelled concentrations is executed. After interpolation, a back-transformation is applied.

Separate map layers are created for rural and urban background areas on a grid at resolution of 1x1 km² (for PM_{10} and NO_2) and 10x10 km² (for ozone), and for urban traffic areas at 1x1 km² (for PM_{10} and NO_2). The rural background map layer is based on rural background stations, the urban background map layer on urban and suburban background stations and the potential urban traffic map layer is based on urban and suburban traffic stations. Subsequently, the separate map layers are merged into one combined final map at 1x1 km² resolution, according to

$$\hat{Z}_F(s_0) = \left(1 - w_U(s_0)\right) \cdot \hat{Z}_R(s_0) + w_U(s_0) \cdot \hat{Z}_{UB}(s_0) \qquad \text{resp.}$$
$$\hat{Z}_F(s_0) = \left(1 - w_U(s_0)\right) \cdot \hat{Z}_R(s_0) + w_U(s_0)\left(1 - w_T(s_0)\right) \cdot \hat{Z}_{UB}(s_0) + w_T(s_0) \cdot \hat{Z}_{UT}(s_0) \qquad (2.3)$$

where $\hat{Z}_F(s_0)$ is the resulting estimated concentration in a grid cell s_o for the final map,
$\hat{Z}_R(s_0)$, $\hat{Z}_{UB}(s_0)$ and $\hat{Z}_{UT}(s_0)$ is the estimated concentration in a grid cell s_o for the rural background, the urban background and urban traffic map layer, respectively
$w_U(s_0)$ is the weight representing the ratio of the urban character of the grid cell s_o.
$w_T(s_0)$ is the weight representing the ratio of areas exposed to traffics in a grid cell s_o.

The weight $w_U(s_0)$ is based on the population density, while the weight $w_T(s_0)$ is based on the buffers around the roads (Section 3.3). For details, see Horálek et al. (2021b and references therein).

2.2 CAMS Modelling Data Products

The Copernicus Atmosphere Monitoring Service (CAMS) is one of six Copernicus services. CAMS provides a diverse range of environmental atmospheric information, which specifically includes the provision of air quality information at a regional scale over Europe. This European regional service is of specific interest for this current work. The European regional production consists of an ensemble of seven (resp. nine since October 2019) air quality models run operationally over the domain outlined in Map 2.1.

Map 2.1. Example map showing the spatial extent of the CAMS European regional air quality domain.

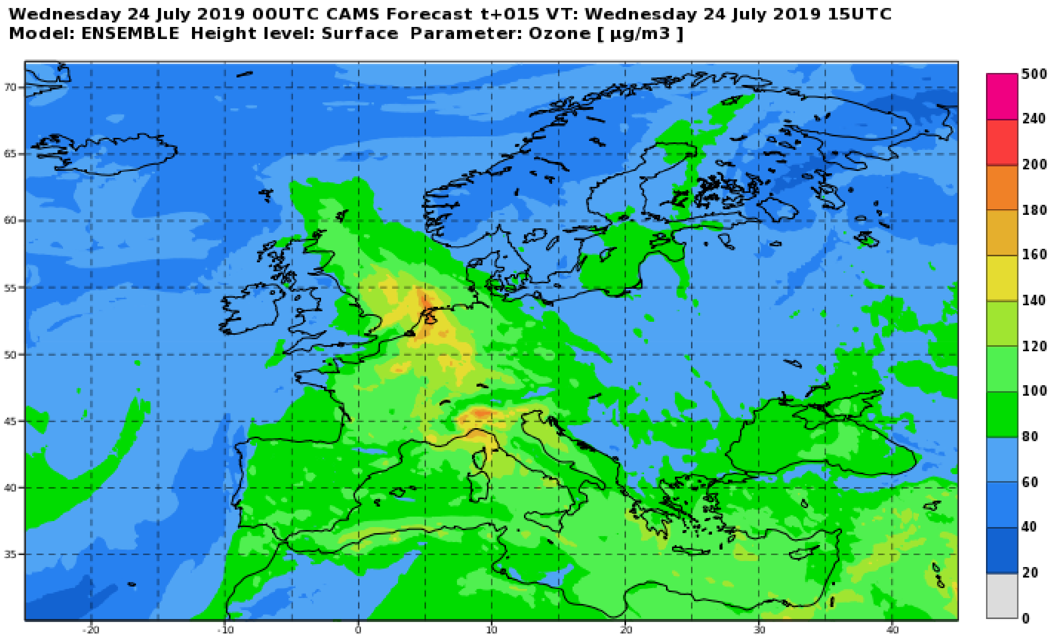

Each model is run by one of different European institutes. The nine different models and the institutes responsible for running each one are summarized in Table 2.1.

Table 2.1. A table summarising the chemistry-transport models used in CAMS and the institutions responsible for running the models

Institute	Model
INERIS, France	CHIMERE
Norwegian Meteorological Institute	EMEP
Rhenish Institute for Environmental Research at the University of Cologne, Germany	EURAD
KNMI/TNO, Netherlands	LOTOS-EUROS
Swedish Meteorological and Hydrological Institute	MATCH
Météo France	MOCAGE
Finnish Meteorological Institute	SILAM
Aarhus University, Denmark	DEHM ([a])
Institute for Environmental Protection – National Research Institute, Poland	GEM-AQ ([a])

([a]) Since October 2019.

All of the models are what are termed as chemical transport models, which means they simulate atmospheric chemistry but rely on an external meteorological model to provide the weather forecast that governs the transport of pollutants in the model. The European Center for Medium Range Weather Forecasts (ECMWF) provides the weather forecast for each of the regional models in CAMS, which ensures that each model is using the same base meteorology. For further details of each model please consult (Marécal et al., 2015).

The models provide (together with other products) a 72-hour forecast made available at 07:00 UTC the day of the forecast. The forecast data product is available on an hourly time resolution and at a spatial resolution of 0.1° x 0.1°, i.e., ca. 10x10 km^2. Each model forecast is combined into an ensemble forecast by taking the median of each of the seven (prior to October 2019) or nine (since October 2019) models.

The individual forecasts from each model are available as separate products as well, but our interest is with the ensemble median product. Extensive validation and verification demonstrate that the ensemble have superior skill compared to any of the individual model ensemble members[1] (Marécal et al., 2015). Thus, for this work, we focus on the use of the CAMS ensemble (CAMS-ENS) products. CAMS is currently running a dedicated project (coordinated by INERIS) to improve this Ensemble product using more elaborated statistical techniques (including machine learning) than this simple median. This improved methodology is scheduled to become operational after 2021.

The use of the ensemble forecast in the air quality mapping means that no information from surface observations is contained in the modelling product. However, the ensemble analysis product is created by assimilating surface observations, and so the modelling product already contains some information from the surface station observations. In terms of the quality of the map, it causes a slight underestimation of the mapping uncertainty.

In this report CAMS modelling data is used in the RIMM spatial mapping. In principle, the CAMS modelling data are used as the chemical transport modelling data in Equation 2.1, instead of routinely used EMEP modelling data.

2.3 Pseudo station data estimation

In order to supplement the E2a measurement data, which are affected by some spatial gaps, in the mapping procedure we also use data from so-called *pseudo stations.* These data are concentration estimates at the locations of stations with no E2a data for the actual year Y, but with the validated E1a data for the year Y-1. As recommended by Horálek et al. (2021a), these estimates are based on the relation between E2a data from year Y and validated E1a data from year Y-1. Based on preliminary analysis, next to the validated E1a data from year Y-1, also the modelling results in the points of these stations in years Y and Y-1 are taken into account in this estimation. Specifically, the ratio of the modelling CAMS-ENS Forecast data (see Section 2.2) in years Y and Y-1 are used. The estimates are calculated based on the equation

$$\hat{Z}_Y(s) = c + a_1 . Z_{Y-1}(s) + a_2 . \frac{M_Y}{M_{Y-1}} . Z_{Y-1}(s) \qquad (2.4)$$

where $\hat{Z}_Y(s)$ is the estimated concentration value at a station *s* for the year *Y*,
$Z_{Y-1}(s)$ is the measurement value at a station *s* for the year *Y-1,* based on the E1a data,
$M_Y(s)$, $M_{Y-1}(s)$ are the modelling data at a station *s* for the years *Y* and *Y-1*,
c, a_1,, a_2 are the parameters of the linear regression model calculated based on the data at the points of all stations with measurements for both *Y* and *Y-1* years.

[1] https://atmosphere.copernicus.eu/regional-services

Similarly as in the case of the pseudo stations used in the regular mapping of $PM_{2.5}$ (see Horálek et al., 2021b), all background stations (either classified as rural, urban or suburban) are handled together for estimating values at background pseudo stations, while all traffic stations used are applied for estimating values at traffic pseudo stations.

2.4 Validation

In this report, we perform the validation of both the pseudo station estimates and the concentration maps.

Pseudo stations

The validation of the pseudo station estimates is done based on the E1a measurement data, if available (i.e., for 2017 data). The statistical indicators for the validation are *standard error* and R^2.

Concentration maps

The validation of the concentration maps is done based on the E1a data, if available (i.e. for 2017). For stations with E1a data only (i.e., with no E2a data), the simple *point observation – grid prediction validation* is performed, which compares between point measurement data *at stations not used in mapping* (as they do not have E2a data) and gridded prediction values of the relevant RIMM map.

For stations with both E2a and E1a data available, the evaluation is done using the *cross-validation*: it computes the spatial interpolation for each measurement point from all available information except from the point in question (i.e., it withholds one data point and then makes a prediction at the spatial location of that point). This procedure is repeated for all measurement points in the available set. The predicted and measurement E1a values at these points are compared using statistical indicators and a scatter plot. For 2019 maps, the cross-validation based on E2a data is performed.

The results of both cross-validation and simple validation are described by the statistical indicators and scatter plots. The main indicator used is root mean squared error (RMSE) and additional is bias (mean prediction error, MPE):

$$RMSE = \sqrt{\frac{1}{N}\sum_{i=1}^{N}\left(\hat{Z}(s_i) - Z(s_i)\right)^2} \qquad (2.5)$$

$$bias(MPE) = \frac{1}{N}\sum_{i=1}^{N}\left(\hat{Z}(s_i) - Z(s_i)\right) \qquad (2.6)$$

where $Z(s_i)$ is the air quality indicator value derived from the measured concentration at the i^{th} point, $i = 1, \ldots, N$,

$\hat{Z}(s_i)$ is the air quality estimated indicator value at the i^{th} point using other information, without the indicator value derived from the measured concentration at the i^{th} point,

N is the number of the measuring points.

Next to the RMSE expressed in the absolute units, one could express this uncertainty in relative terms by relating the RMSE to the mean of the air pollution indicator value for all stations:

$$RRMSE = \frac{RMSE}{\bar{Z}}.100 \qquad (2.7)$$

where $RRMSE$ is the relative RMSE, expressed in percent,

$\bar{Z}$ is the arithmetic average of the indicator values $Z(s_1), \ldots, Z(s_N)$, as derived from measurement concentrations at the station points $i = 1, \ldots, N$.

Other indicators are R^2 and the regression equation parameters *slope* and *intercept*, following from the scatter plot between the predicted (using cross-validation) and the observed concentrations.

RMSE should be as small as possible, bias (MPE) should be as close to zero as possible, R^2 should be as close to *1* as possible, slope *a* should be as close to *1* as possible, and intercept *c* should be as close to zero as possible (in the regression equation $y = a.x + c$).

3 Data Used

3.1 Air Quality Monitoring Data

AQ e-reporting E2a and E1a data

For the preliminary maps, we have used air quality station monitoring data coming from the E2a data set of the Air Quality e-Reporting database (EEA, 2020). The data of the up-to-date (UTD) dataflow E2a are being provided on an hourly basis from most of the EEA's member and cooperating countries.The data for 2017 was extracted by the EEA in the first half of the year 2018 and the data for 2019 was extracted by the EEA in February 2020.

For the purposes of the pseudo stations calculations and for the validation of the interim maps, the data of the E1a data set of the Air Quality e-Reporting database (EEA, 2020) have been used. The data of the dataflow E1a is submitted to EEA by the reporting countries every September and covers the year before the delivery. This E1a data set has been supplemented with several EMEP rural stations from the database EBAS (NILU, 2020) not reported to the Air Quality e-Reporting database.

For PM_{10} and NO_2, and also for $PM_{2.5}$, we use the same classification types of stations and areas as we do for the E2a data, i.e. stations classified as background (for the three types of area), and also traffic for the types of area suburban and urban. For ozone, we use only data from stations classified as background (for the three types of area, rural, suburban and urban). In the mapping, rural background stations are used for the rural layer, urban and suburban stations for the urban background layer and urban and suburban traffic stations for the urban traffic layer (Section 2.1).

The following pollutants and aggregations are considered:

PM_{10} – annual average [$\mu g \cdot m^{-3}$], years 2016 (E1a), 2017 (E1a, E2a), 2018 (E1a), 2019 (E2a)
Ozone – SOMO35 [$\mu g \cdot m^{-3} \cdot d$], years 2016 (E1a), 2017 (E1a, E2a), 2018 (E1a), 2019 (E2a)
NO_2 – annual average [$\mu g \cdot m^{-3}$], years 2016 (E1a), 2017 (E1a, E2a), 2018 (E1a), 2019 (E2a)
$PM_{2.5}$ – annual average [$\mu g \cdot m^{-3}$], years 2016 (E1a), 2017 (E1a, E2a)

Table 3.1 shows the number of the stations used in both mapping and validation of 2017 and 2019 interim maps. Validation is performed in the year 2017 only, based on the E1a stations.

Note that due to a low number of the E2a data in 2017, the $PM_{2.5}$ mapping has not been performed (Section 4.4). Consequently, we have not prepared the $PM_{2.5}$ map for 2019.

In the RIMM mapping (as described in Section 2.1) of a year Y, E2a Y stations are used, together with pseudo stations derived from E1a stations of a year a Y-1. The pseudo stations are located at the places of the E1a Y-1 stations with no E2a data for year Y (labelled as "For pseudo Y"). The rest of the E1a Y-1 stations (with both E1a data for Y-1 and E2a data for Y) are used for estimation of the parameters of the linear regression for the pseudo stations calculation (see Eq. 2.4).

Table 3.1 Number of stations used in interim mapping 2017 and 2019 and validation 2017 for each station type, for PM_{10} (top), NO_2 (upper middle), ozone (lower middle) and $PM_{2.5}$ (bottom)

Station type	PM_{10}						
	E1a 2016		E2a 2017	E1a 2017	E1a 2018		E2a 2019
	Total	For pseudo ´17	Mapping ´17	Validation ´17	Total	For pseudo ´19	Mapping ´19
Rural background	351	169	193	362	386	156	237
Urban/suburban backgr.	1313	695	670	1386	1422	618	848
Urban/suburban traffic	685	358	355	746	758	287	494

Station type	NO_2						
	E1a 2016		E2a 2017	E1a 2017	E1a 2018		E2a 2019
	Total	For pseudo ´17	Mapping ´17	Validation ´17	Total	For pseudo ´19	Mapping ´19
Rural background	429	156	285	451	480	151	343
Urban/suburban backgr.	1303	491	842	1336	1381	349	1071
Urban/suburban traffic	787	302	511	975	1060	426	654

Station type	Ozone						
	E1a 2016		E2a 2017	E1a 2017	E1a 2018		E2a 2019
	Total	For pseudo ´17	Mapping ´17	Validation ´17	Total	For pseudo ´19	Mapping ´19
Rural background	531	156	375	532	551	121	440
Urban/suburban backgr.	1145	387	785	1133	1201	328	902

Station type	$PM_{2.5}$			
	E1a 2016		E2a 2017	E1a 2017
	Total	For pseudo ´17	Mapping ´17	Validation ´17
Rural background	195	113	90	201
Urban/suburban backgr.	631	338	323	686
Urban/suburban traffic	303	146	176	330

Maps A.1-A.3 of Annex show the spatial distribution of the rural, urban/suburban background and urban/suburban traffic stations used in the interim 2017 mapping (in green and orange) and validation (in red), for different pollutants. In all figures, the true stations (in green) and the pseudo stations (in orange) are distinguished. Similarly, Maps A.4-A.6 of Annex present the spatial distribution of the stations of the different types used in the interim 2019 mapping (in green and orange).

3.2 Chemical transport modelling data

CAMS Ensemble Forecast Modelling Data

We use the CAMS Ensemble Forecast data, see Section 2.2. We have downloaded the CAMS Ensemble Forecast data for 2016, 2017, 2018 and 2019 from the CAMS data archive[2]. The modelling data have been downloaded in NetCDF format.

The forecast products are available at hourly intervals and have a spatial resolution of $0.1 \times 0.1°$. All of the models used in the CAMS ensemble products were run using the TNO-MACC emissions representative of 2011 (Kuenen et al., 2014). The CAMS ensemble modelling products are described in further detail in Section 2.2.

All modelling data have been aggregated into the annual statistics and converted into the reference EEA 1x1 km^2 (for PM and NO_2) and 10x10 km^2 (for ozone) grids. The pollutants and parameters used are the same as for the monitoring data.

3.3 Other supplementary data

Other supplementary data used are similar as in regular maps creation, Horálek et al. (2020, 2021b).

[2] http://www.regional.atmosphere.copernicus.eu/?category=data_access

Altitude

We use the altitude data field (in m) of Global Multi-resolution Terrain Elevation Data 2010 (GMTED2010), with an original grid resolution of 15x15 arcseconds coming from U.S. Geological Survey Earth Resources Observation and Science, see Danielson et al. (2011). The data were converted into the EEA reference grids in 1x1 km^2 and 10x10 km^2 resolutions, as described in Horálek et al. (2020). Next to this, another aggregation has been executed based on the 1x1 km^2 grid cells, i.e., the floating average of the circle with a radius of 5 km around all relevant grid cells.

Meteorological data

The meteorological parameters used are *wind speed* (annual mean for 2017 and for 2019, in $m.s^{-1}$), *relative humidity* (annual mean for 2017 and for 2019, in percent) and *surface net solar radiation* (annual mean of daily sum for 2017 and for 2019, in $MWs.m^{-2}$). For 2017, the daily data in resolution 15x15 arc-seconds were extracted from the Meteorological Archival and Retrieval System (MARS) of ECMWF. For 2019, the ECWMF hourly data in 0.1°x0.1° resolution extracted from the CDS (Climate Data Store, https://cds.climate.copernicus.eu/cdsapp#!/home) are used. The data have been imported into ArcGIS and converted into the reference EEA 1x1 km^2 and 10x10 km^2 grids.

Satellite data

Annual average NO_2 datasets from data acquired by the Ozone Monitoring Instrument (OMI) onboard the Aura platform were constructed for 2017. The parameter used is the annual average tropospheric vertical column density (VCD) [number of NO_2 molecules per cm^2 of earth surface], aggregated from daily data. The OMI Level-3 NO_2 product "OMNO2d" was used as a basis, NASA (2020). All the orbits within a given day (typically observed between 13:00 and 14:00 local time) are mapped into a 0.25°x0.25° grid resolution. For details, see Horálek et al. (2020). The data were spatially transformed to the reference EEA 1x1 km^2 grid, like in the case of modelled data.

For 2019 mapping, data from the TROPOspheric Monitoring Instrument (TROPOMI) onboard of the Sentinel-5 Precursor satellite was used. The spatial resolution of approximately 7 km by 3.5 km at nadir was reduced to 5.5 km by 3.5 km after August 2019. The product used is the S5P_OFFL_L2__NO2 product (van Geffen et al., 2020) and it provides the tropospheric vertical column density of nitrogen dioxide (NO_2), i.e., a vertically integrated value over the entire troposphere. All overpasses for a specific day were then mosaicked and gridded into the reference EEA 1x1 km^2 grid in the ETRS89 / ETRS-LAEA (EPSG 3035) projection. The daily gridded files were subsequently averaged to an annual mean.

Land cover

CORINE Land Cover 2012 – grid 100 x 100 m^2, Version 18.5 (EEA, 2016) is used for 2017 maps, while CORINE Land Cover 2018 – grid 100 x 100 m^2, Version 2020_20 (EU, 2020) for 2019 maps. Like in Horálek et al. (2021b), the 44 CLC classes have been re-grouped into the 8 more general classes. In this paper, we use five of these general classes, namely high density residential areas (HDR), low density residential areas (LDR), agricultural areas (AGR), natural areas (NAT), and traffic areas (TRA). For details, see Horálek et al. (2021b). Two aggregations are used, i.e., into 1x1 km^2 grid and into the circle with radius of 5 km. The aggregated grid square value represents for each general class the total area of this class as percentage of the total area of the 1x1 km^2 square or the circle with radius of 5 km.

Population density and Road data

Population density (in $inhabitants.km^{-2}$, census 2011) is based on Geostat 2011 grid dataset (Eurostat, 2014). For regions not included in the Geostat 2011 dataset we use as alternative sources JRC and ORNL data. For details, see Horálek et al. (2021b).

GRIP vector road type data is used (Meijer et al., 2018). Based on these data (i.e., buffers around the roads), traffic map layers (Section 2.1) are merged into the final maps (Horálek et al., 2021b).

4 Evaluation of Interim Air Quality Spatial Mapping for 2017

4.1 PM_{10} Annual Average

As a first step, the pseudo stations data have been estimated. The estimates have been calculated based on the E1a measurement data for 2016, the CAMS Ensemble Forecast modelling data for 2016 and 2017, and the regression relation with the E2a measurement data for 2017 (see Eq. 2.4). Table 4.1 presents the regression coefficients determined for pseudo stations data estimation, based on the 800 rural and urban/suburban background and 327 urban/suburban traffic stations that have both E1a 2016 and E2a 2017 measurements available (see Section 2.2).

Table 4.1 Parameters and statistics of linear regression model for generation of pseudo PM_{10} data in rural and urban background and urban traffic areas, for PM_{10} annual average 2017

PM_{10}		Rural and urban background areas	Urban traffic areas
Linear regression model (LRM, Eq. 2.4)	c (constant)	-0.3	2.6
	a1 (PM_{10} annual mean 2016, E1a data)	0.366	0.577
	a2 (PM_{10} annual mean 2016 * CAMS ratio 2019/2018)	0.693	0.323
	Adjusted R^2	**0.92**	**0.84**
	Standard Error [μg.m^{-3}]	**2.1**	**3.1**

Table 4.2 shows the validation of the pseudo stations, based on the E1a stations not included in the E2a data set. The validation has been performed separately for rural, urban/suburban background and urban/suburban traffic stations. Next to this, the validation has been executed separately for areas covered by the E2a data (i.e., for entire area without Italy, Bulgaria, Romania, Serbia, Baltic countries, Cyprus and Turkey) and not covered by the E2a data (i.e., for Italy, Bulgaria, Romania, Serbia, Baltic countries, Cyprus and Turkey). Additionally, for areas not covered by the E2a data, we show separately the urban background results for areas outside Turkey and for Turkey, due to much higher uncertainty for Turkey compared to the other areas (similarly like in regular maps, Horálek et al., 2020a).

Table 4.2 Validation of pseudo PM_{10} data showing RMSE, RRMSE, bias, R^2 and linear regression from validation scatter plots for rural background (top), urban/suburban background (middle) and urban/suburban traffic stations (bottom), PM_{10} annual mean 2017. Validation by E1a stations not used in mapping. Units: μg.m^{-3} except RRMSE and R^2.

PM_{10} – Rural background stations						
Validation set	**Area**	**RMSE**	**RRMSE**	**Bias**	**R^2**	**Regr. eq.**
E1a stations not in E2a data set	Entire area	2.9	16.5%	-0.2	0.874	y = 0.874x + 2.00
	Area covered by E2a data	1.8	12.4%	0.3	0.880	y = 0.961x + 0.84
	Area not covered by E2a data	3.9	18.5%	-0.8	0.851	y = 0.854x + 2.27
PM_{10} - Urban/suburban background stations						
Validation set	**Area**	**RMSE**	**RRMSE**	**Bias**	**R^2**	**Regr. eq.**
E1a stations not in E2a data set	Entire area	7.1	22.9%	0.5	0.818	y = 0.959x + 1.79
	Area covered by E2a data	3.0	12.4%	0.6	0.926	y = 1.063x - 0.91
	Area not covered by E2a data, no TR	3.0	11.5%	-0.4	0.851	y = 0.858x + 3.33
	Area not covered by E2a data, TR	14.1	27.7%	1.8	0.512	y = 0.765x + 13.83
PM_{10} – Urban/suburban traffic stations						
Validation set	**Area**	**RMSE**	**RRMSE**	**Bias**	**R^2**	**Regr. eq.**
E1a stations not in E2a data set	Entire area	4.3	16.1%	-0.7	0.892	y = 0.848x + 3.32
	Area covered by E2a data	2.1	10.2%	0.3	0.918	y = 0.897x + 2.41
	Area not covered by E2a data	5.5	17.3%	-1.6	0.860	y = 0.842x + 3.44

Note: Areas not covered by E2a data are comprised of IT, BG, RO, RS, LT, LV, EE, CY and TR.

Observing the validation results, one can see that apart from the area of Turkey, the bias is mostly smaller than 1 µg.m^{-3}, the R^2 is higher than 0.85 and the relative uncertainty RRMSE is smaller than 20 %, for all types of the area.

Based on the E2a data and pseudo data, CAMS Ensemble Forecast modelling data and other supplementary data as used in the regular mapping, the interim PM_{10} annual average map for 2017 has been created.

Table 4.3 presents the estimated parameters of the linear regression models (*c, a_1, a_2,…*) and of the residual kriging (*nugget, sill, range*) and includes the statistical indicators of both the regression and the kriging of its residuals.

Table 4.3 Parameters and statistics of linear regression model and ordinary kriging in rural, urban background and urban traffic areas for interim map of PM_{10} annual average 2017

PM_{10}		**Annual average**		
		Rural areas	**Urban b. areas**	**Urban tr.. areas**
Linear regresion model (LRM, Eq. 2.1)	c (constant)	5.42	1.19	2.10
	a1 (log. CAMS-ENS-FC model)	0.746	0.79	0.522
	a2 (altitude GMTED)	-0.00025		
	a3 (relative humidity)	*n.sign.*		
	a4 (wind speed)	-0.046		-0.063
	a5 (land cover NAT1)	-0.0019		
	Adjusted R^2	**0.65**	**0.28**	**0.42**
	Standard Error [µg.m^{-3}]	**0.26**	**0.38**	**0.26**
Ordinary kriging (OK) of LRM residuals	nugget	0.031	0.041	0.010
	sill	0.065	0.077	0.043
	range [km]	760	740	480
LRM + OK of its residuals	**RMSE [µg.m^{-3}]**	**4.0**	**3.8**	**4.3**
	Relative RMSE [%]	**26.3%**	**18.9%**	**19.5%**
	Bias (MPE) [µg.m^{-3}]	**-0.1**	**0.3**	**-0.3**

Table 4.4 presents the evaluation of the interim map, based on the E1a station data not included in the E2a data set, for different areas types. Next to the analysis for the entire mapping area, we have again executed the comparison separately for two distinct areas: for areas covered and not covered by the E2a data. Additionally, for areas not covered by the E2a data, we show separately the urban results for areas outside Turkey and for Turkey, due to much higher uncertainty for Turkey compared to the other areas (similarly like in regular maps, Horálek et al., 2020).

Next to the results for the final interim map, the results for the specific map layers (i.e., rural, urban background and urban traffic) are also presented. Note that as stated in Horálek et al. (2021b), the final combined map in 1x1 km^2 resolution is fairly well representative for rural and urban background areas, but not for urban traffic areas. Thus, for urban traffic areas, results for the traffic map layer is decisive, while the results for the final map are presented for completeness only.

Lower RMSE and RRMSE and higher R^2 generally indicate better performance; bias closer to zero is also an indication of better performance. Furthermore, the slope should be as close to *1* as possible and the intercept as close to *0* as possible.

Looking at the statistics, one can state that the results are quite satisfactory in general. Comparing with the results presented in Horálek et al. (2021a) for the interim maps without the use of the pseudo stations, one can see quite similar results in areas covered by the E2a data and altogether better results in areas not covered by the E2a data. The most remarkable improvement is in R^2.

Table 4.4 Validation of interim RIMM spatial mapping showing RMSE, RRMSE, bias, R^2 and linear regression from validation scatter plots for PM_{10} annual mean in rural background (top), urban background (middle) and urban traffic areas (bottom), 2017. Cross-validation and validation by E1a stations not used in mapping. Units: µg.m^{-3} except RRMSE and R^2.

PM_{10} – Rural background areas								
Validation set	**Area**	**Type of valid.**	**Type of map**	**RMSE**	**RRMSE**	**Bias**	**R^2**	**Regr. eq.**
E1a stations in E2a set	Area covered by E2a data	Cross-validation	Rural map layer	2.5	16.8%	0.1	0.739	y = 0.697x + 4.58
E1a stations not in E2a data set	Entire area	Simple grid validation	Rural map layer	3.4	20.1%	-0.2	0.837	y = 0.746x + 4.15
			Final merged map	4.9	29.0%	1.0	0.694	y = 0.861x + 3.33
	Area covered by E2a data	Simple grid validation	Rural map layer	2.6	17.8%	0.4	0.797	y = 0.793x + 3.34
			Final merged map	2.8	19.4%	0.9	0.784	y = 0.839x + 3.19
	Area not covered by E2a data	Simple grid validation	Rural map layer	4.4	21.0%	-1.0	0.819	y = 0.839x + 3.19
			Final merged map	7.1	33.6%	1.1	0.580	y = 0.819x + 4.5

PM_{10} – Urban background areas								
Validation set	**Area**	**Type of valid.**	**Type of map**	**RMSE**	**RRMSE**	**Bias**	**R^2**	**Regr. eq.**
E1a stations in E2a set	Area covered by E2a data	Cross-validation	Urban b. map layer	3.6	17.9%	0.5	0.764	y = 0.807x + 4.40
E1a stations not in E2a data set	Entire area	Simple grid validation	Urban b. map layer	8.4	28.0%	-0.4	0.686	y = 0.675x + 9.35
			Final merged map	8.7	29.2%	-0.7	0.660	y = 0.673x + 9.13
	Area covered by E2a data	Simple grid validation	Urban b. map layer	4.3	17.8%	-0.2	0.800	y = 0.781x + 5.14
			Final merged map	4.4	18.1%	-0.4	0.796	y = 0.775x + 5.13
	Area not covered by E2a data, no TR	Simple grid validation	Urban b. map layer	5.1	19.2%	-0.1	0.612	y = 0.663x + 8.75
			Final merged map	5.3	20.0%	-0.7	0.594	y = 0.678x + 7.81
	Area not covered by E2a data, TR	Simple grid validation	Urban b. map layer	16.9	33.5%	-1.3	0.171	y = 0.186x + 39.70
			Final merged map	17.7	35.1%	-1.2	0.110	y = 0.156x + 41.24

PM_{10} – Urban traffic areas								
Validation set	**Area**	**Type of valid.**	**Type of map**	**RMSE**	**RRMSE**	**Bias**	**R^2**	**Regr. eq.**
E1a stations in E2a set	Area covered by E2a data	Cross-validation	Urban tr. map layer	3.9	17.6%	-0.4	0.763	y = 0.681x + 6.58
E1a stations not in E2a data set	Entire area	Simple grid validation	Urban tr. map layer	4.8	18.5%	-0.6	0.849	y = 0.775x + 5.32
			Final merged map	6.5	25.1%	-3.1	0.775	y = 0.754x + 3.32
	Area covered by E2a data	Simple grid validation	Urban tr. map layer	3.3	16.5%	0.1	0.595	y = 0.697x + 6.52
			Final merged map	5.3	26.1%	-3.0	0.515	y = 0.720x + 2.82
	Area not covered by E2a data	Simple grid validation	Urban tr. map layer	5.9	18.7%	-1.1	0.820	y = 0.721x + 7.66
			Final merged map	7.5	23.8%	-3.3	0.749	y = 0.651x + 7.77

Note: Areas not covered by E2a data are comprised of IT, BG, RO, RS, LT, LV, EE, CY and TR.

Map 4.1 presents the final merged interim map of the PM_{10} annual average for 2017.

Map 4.2 shows difference map between the interim map and the reference map (Horálek et al., 2020).

From Map 4.2, one can see overall agreement of the two maps (i.e. the interim and regular ones), with regional differences in some areas, including Hungary, Spain, Poland and Turkey. The differences are partly caused by changes in the measurement data coverage, partly by the different model used (i.e. CAMS Ensemble Forecast instead of EMEP). Compared with the results presented in Horálek et al. (2021a), one can see an improvement in areas poorly covered by the E2a stations (namely in Balkan, Italy and Scandinavia).

Map 4.1 Interim concentration map of PM_{10} annual average, 2017, RIMM methodology using E2a (UTD) measurement data, pseudo data and CAMS-ENS Forecast model output

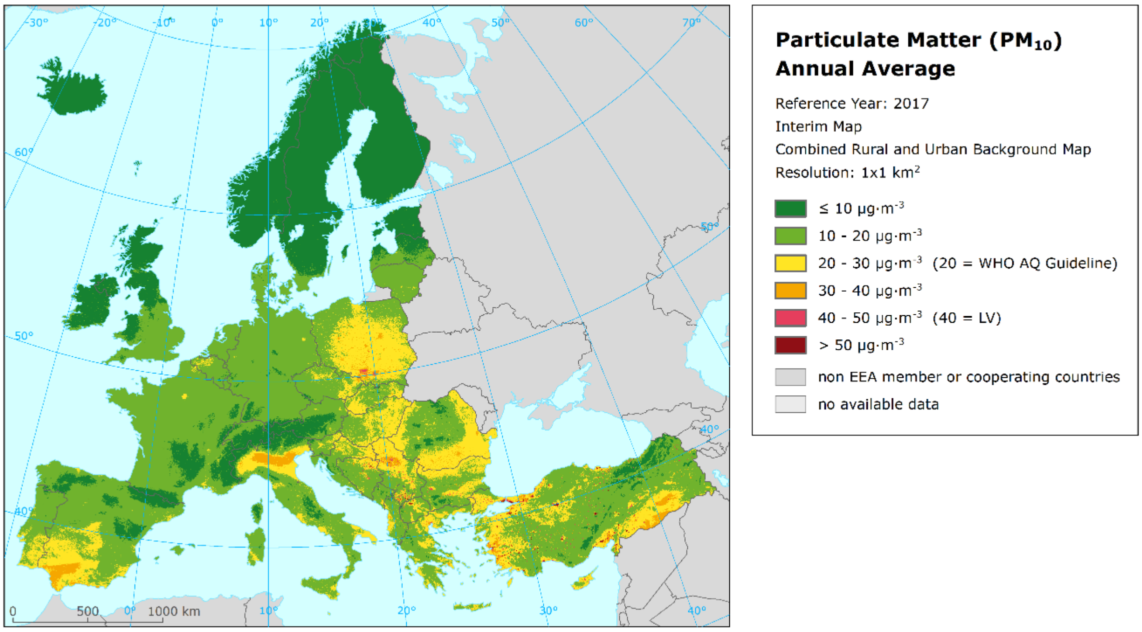

Map 4.2 Difference map of PM_{10} annual average, 2017, interim map using E2a measurement, pseudo data and CAMS-ENS Forecast model data minus reference map using E1a measurement and EMEP model data

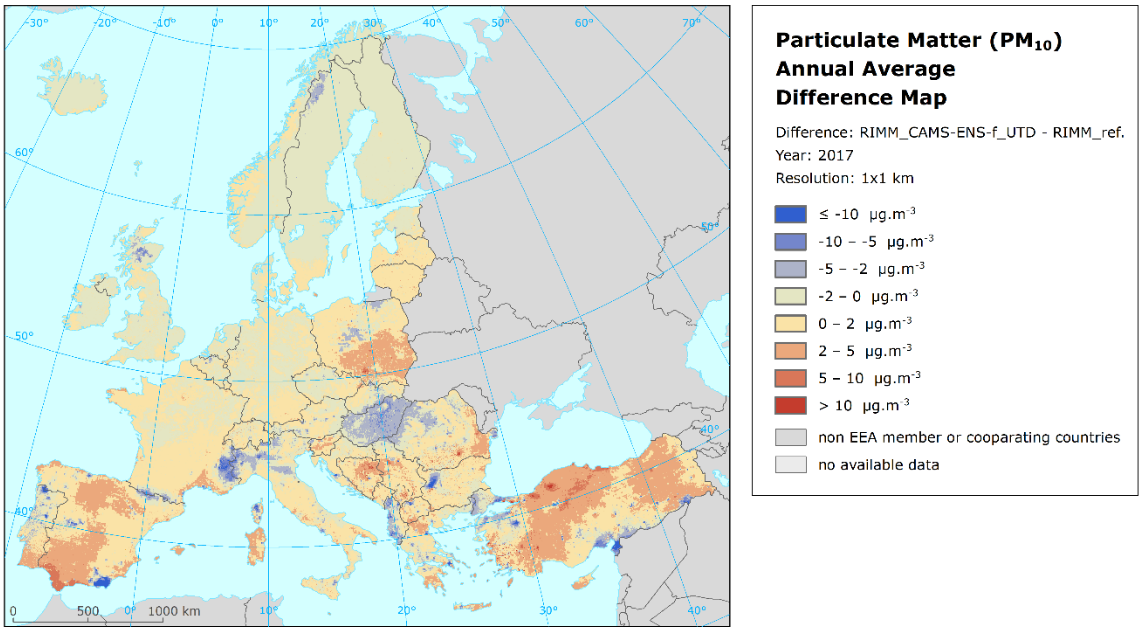

It can be concluded that the uncertainty of the map (see the relative uncertainty expressed as RRMSE, Table 4.4) is low enough to enable the interim map construction (e.g., it fulfils the data quality objectives for models as set in the AQ Directive, EC, 2008). However, two notes should be made.

The first comment is that for the area of Turkey (covered with no E2a data) the uncertainty results for urban background areas still are not satisfactory (see R^2 lower than 0.2), although the results are better compared to those of Horálek et al (2021a). Also, only few pseudo stations are available for rural and traffic areas. This leads to the recommendation not to present the interim mapping results for the area of Turkey, for the time being. Second, slightly higher bias compared to the regular map can be seen for the most types of areas. This should not be a problem for the mapping itself, however, together with a regional variability compared to the regular mapping, it leads to the recommendation concerning the population exposure (not examined in this report), which are more sensitive to any bias: the population exposure estimates should be not be routinely calculated before being properly analysed.

4.2 NO_2 Annual Average

Like for PM_{10}, we have performed the analysis for the interim NO_2 annual average 2017 map creation.

At first, the pseudo stations data have been estimated, based on the E1a measurement data for 2016, the CAMS Ensemble Forecast modelling data for 2016 and 2017, and the regression relation with the E2a measurement 2017 data. It should be noted that based on the preliminary analysis (not presented here), it seems that, instead of the CAMS modelling data, the OMNO2 satellite data (for 2016 and 2017) might be used alternatively for the pseudo data estimates.

Table 4.5 presents the regression coefficients determined for pseudo stations data estimation, based on the 1085 rural and urban/suburban background and 485 urban/suburban traffic stations that have both E1a 2016 and E2a 2017 measurements available (Section 2.2). R^2 above 0.9 means a good relation.

Table 4.5 Parameters and statistics of linear regression model for generation of pseudo NO_2 data in rural and urban background and urban traffic areas, for NO_2 annual average 2017

NO_2		Rural and urban background areas	Urban traffic areas
Linear regression model (LRM, Eq. 2.4)	c (constant)	-0.1	2.0
	a1 (NO_2 annual mean 2016, E1a data)	0.650	0.670
	a2 (NO_2 annual mean 2016 * CAMS ratio 2017/2016)	0.344	0.237
	Adjusted R^2	**0.95**	**0.93**
	Standard Error [$\mu g.m^{-3}$]	**1.8**	**3.3**

Table 4.6 shows the validation of the pseudo data, using E1a stations not included in the E2a data set.

Table 4.6 Validation of pseudo NO_2 data showing RMSE, RRMSE, bias, R^2 and linear regression from validation scatter plots for rural background (top), urban/suburban background (middle) and urban/suburban traffic stations (bottom), NO_2 annual mean 2017. Validation by E1a stations not used in mapping. Units: $\mu g.m^{-3}$ except RRMSE and R^2.

NO_2 – Rural background stations						
Validation set	**Area**	**RMSE**	**RRMSE**	**Bias**	**R^2**	**Regr. eq.**
E1a stations not in E2a data set	Entire area	1.5	14.3%	-0.5	0.963	y = 0.950x + 0.07
	Area covered by E2a data	1.0	12.1%	-0.3	0.980	y = 0.937x + 0.27
	Area not covered by E2a data	1.7	14.8%	-0.6	0.954	y = 0.959x - 0.09
NO_2 - Urban/suburban background stations						
Validation set	**Area**	**RMSE**	**RRMSE**	**Bias**	**R^2**	**Regr. eq.**
E1a stations not in E2a data set	Entire area	8.0	33.9%	-0.1	0.679	y = 0.973x + 0.50
	Area covered by E2a data	2.0	11.0%	-0.1	0.907	y = 0.922x + 1.27
	Area not covered by E2a data, no TR	3.4	14.6%	-1.1	0.862	y = 0.908x + 1.05
	Area not covered by E2a data, TR	3.7	55.5%	3.7	0.365	y = 0.869x + 8.34
NO_2 – Urban/suburban traffic stations						
Validation set	**Area**	**RMSE**	**RRMSE**	**Bias**	**R^2**	**Regr. eq.**
E1a stations not in E2a data set	Entire area	5.9	17.0%	1.0	0.843	y = 0.823x + 5.12
	Area covered by E2a data	3.0	10.3%	0.3	0.919	y = 0.898x + 3.33
	Area not covered by E2a data	6.9	18.4%	-1.7	0.817	y = 0.813x + 5.29

Note: Areas not covered by E2a data are comprised of IT, BG, RO, RS, CY and TR.

Looking at the validation results, one can see that apart from the area of Turkey, the bias is mostly smaller than 1 µg.m^{-3}, the R^2 is higher than 0.85 and the relative uncertainty RRMSE is smaller than 20 %, for all types of the area. The pseudo data show quite similar uncertainty for NO_2 as for PM_{10}.

Based on the E2a data and pseudo data, CAMS Ensemble Forecast modelling data and other supplementary data as used in the regular mapping, the interim NO_2 annual average map for 2017 has been created.

Table 4.7 presents the estimated parameters of the linear regression models (*c, a_1, a_2,…*) and of the residual kriging (*nugget, sill, range*) and includes the statistical indicators of both the regression and the kriging of its residuals.

Table 4.7 Parameters and statistics of linear regression model and ordinary kriging in rural, urban background and urban traffic areas for interim map of NO_2 annual average 2017

NO_2		**Annual average**		
		Rural areas	**Urb. b. areas**	**Urb. tr. areas**
Linear regression model (LRM, Eq. 2.1)	c (constant)	6.7	22.1	26.11
	a1 (CAMS-ENS-FC model)	0.651	0.581	*0.562*
	a2 (satellite OMNO2)	0.35	*n. sign.*	*n. sign.*
	a3 (altitude)	-0.0101	*n. sign.*	*n. sign.*
	a4 (altitude_5km_radius)	0.0101	*n. sign.*	*n. sign.*
	a5 (wind speed)	-0.86	-2.576	-1.699
	a7 (population*1000)	0.00236	0.00032	
	a8 (NAT_1km)		-0.0725	
	a9 (AGR_1km)		-0.0336	
	a10 (TRAF_1km)		0.1008	
	a11 (LDR_5km_radius)	0.0681	*n. sign.*	0.2018
	a12 (HDR_5km_radius)		0.1180	0.2953
	a13 (NAT_5km_radius)	-0.0368		
	Adjusted R^2	**0.80**	**0.39**	**0.37**
	Standard Error [µg.m^{-3}]	**2.6**	**7.9**	**10.0**
Ordinary kriging (OK) of LRM residuals	nugget	6	22	48
	sill	6	26	87
	range [km]	170	90	350
LRM + OK of its residuals	**RMSE [µg.m^{-3}]**	**2.3**	**4.4**	**8.2**
	Relative RMSE [%]	**27.1%**	**22.6%**	**24.7%**
	Bias (MPE) [µg.m^{-3}]	**0.0**	**-0.1**	**0.0**

Table 4.8 presents the evaluation of the interim map, based on the E1a station data not included in the E2a data set, for different areas types. Like for PM_{10}, next to the analysis for the entire mapping area, separate comparison for two distinct areas we have been executed: first, for areas covered by E2a data (i.e., without Italy, Bulgaria, Romania, Serbia, Cyprus and Turkey) and for areas not covered by the E2a data (i.e., for Italy, Bulgaria, Romania, Serbia, Cyprus and Turkey). Like in the case of PM_{10} and in Horálek et al. (2021a), for urban background areas not covered by the E2a data, we present the results separately for areas outside Turkey and for Turkey.

The uncertainty results are quite satisfactory in general. Rural areas show somewhat poorer results compared to the urban background and urban traffic areas, however be it noted that this relative uncertainty is influenced by a low concentration level in rural areas. Similarly like in the case of PM_{10}, large uncertainty can be seen for the urban areas of Turkey (with no E2a data), namely in terms of bias.

Comparing the results with the ones presented in Horálek et al. (2021a) for the interim maps without the use of the pseudo stations, one can see an improvement in urban areas not covered by the E2a data, namely in terms of bias and R^2.

Table 4.8 Validation of interim RIMM spatial mapping showing RMSE, RRMSE, bias, R^2 and linear regression from validation scatter plots for NO_2 annual mean 2017 in rural background (top), urban background (middle) and urban traffic areas (bottom). Cross-validation and validation by E1a stations not used in mapping. Units: µg.m^{-3} except RRMSE and R^2.

NO_2 – Rural background areas								
Validation set	**Area**	**Type of valid.**	**Type of map**	**RMSE**	**RRMSE**	**Bias**	**R^2**	**Regr. eq.**
E1a stations in E2a set	Area covered by E2a data	Cross-validation	Rural map layer	2.2	26.2%	0.0	0.796	y = 0.814x + 1.56
E1a stations not in E2a data set	Entire area	Simple grid validation	Rural map layer	2.9	32.8%	-0.3	0.839	y = 0.790x + 1.55
			Final merged map	4.4	50.0%	0.7	0.663	y = 0.816x + 2.36
	Area covered by E2a data	Simple grid validation	Rural map layer	2.2	34.0%	-0.2	0.876	y = 0.852x + 0.79
			Final merged map	2.5	38.3%	0.1	0.842	y = 0.879x + 0.90
	Area not covered by E2a data	Simple grid validation	Rural map layer	3.4	31.2%	-0.4	0.790	y = 0.725x + 2.56
			Final merged map	5.6	51.4%	1.3	0.510	y = 0.701x + 4.52

NO_2 – Urban background areas								
Validation set	**Area**	**Type of valid.**	**Type of map**	**RMSE**	**RRMSE**	**Bias**	**R^2**	**Regr. eq.**
E1a stations in E2a set	Area covered by E2a data	Cross-validation	Urban b. map layer	4.3	22.1%	-0.1	0.664	y = 0.714x + 5.53
E1a stations not in E2a data set	Entire area	Simple grid validation	Urban b. map layer	7.5	33.3%	0.6	0.565	y = 0.620x + 9.16
			Final merged map	7.9	35.4%	0.4	0.531	y = 0.660x + 7.97
	Area covered by E2a data	Simple grid validation	Urban b. map layer	3.8	21.8%	0.6	0.686	y = 0.666x + 6.52
			Final merged map	4.1	23.3%	1.1	0.666	y = 0.742x + 5.73
	Area not covered by E2a data, no TR	Simple grid validation	Urban b. map layer	6.2	27.7%	-0.4	0.563	y = 0.517x + 10.45
			Final merged map	6.8	30.2%	-1.2	0.503	y = 0.577x + 8.22
	Area not covered by E2a data, TR	Simple grid validation	Urban b. map layer	15.4	44.9%	5.6	0.317	y = 0.296x + 29.79
			Final merged map	16.1	46.7%	6.2	0.279	y = 0.319x + 29.59

NO_2 – Urban traffic areas								
Validation set	**Area**	**Type of valid.**	**Type of map**	**RMSE**	**RRMSE**	**Bias**	**R^2**	**Regr. eq.**
E1a stations in E2a set	Area covered by E2a data	Cross-validation	Urban tr. map layer	8.2	24.5%	-0.2	0.551	y = 0.560x + 14.56
E1a stations not in E2a data set	Entire area	Simple grid validation	Urban tr. map layer	7.9	22.1%	-1.1	0.669	y = 0.599x + 13.21
			Final merged map	14.5	40.8%	3.4	0.564	y = 0.485x + 6.89
	Area covered by E2a data	Simple grid validation	Urban tr. map layer	6.7	19.3%	-0.5	0.666	y = 0.642x + 11.93
			Final merged map	14.3	41.4%	-12.0	0.579	y = 0.430x + 7.71
	Area not covered by E2a data	Simple grid validation	Urban tr. map layer	9.0	24.5%	-1.9	0.676	y = 0.572x + 13.92
			Final merged map	14.8	40.2%	-10.8	0.565	y = 0.510x + 7.22

Note: Areas not covered by E2a data are comprised of IT, BG, RO, RS, CY and TR.

Map 4.3 presents the final merged interim map of the NO_2 annual average for 2017.

Map 4.3 Interim concentration map of NO_2 annual average, 2017, RIMM methodology using E2a (UTD) measurement data, pseudo data and CAMS-ENS Forecast model output

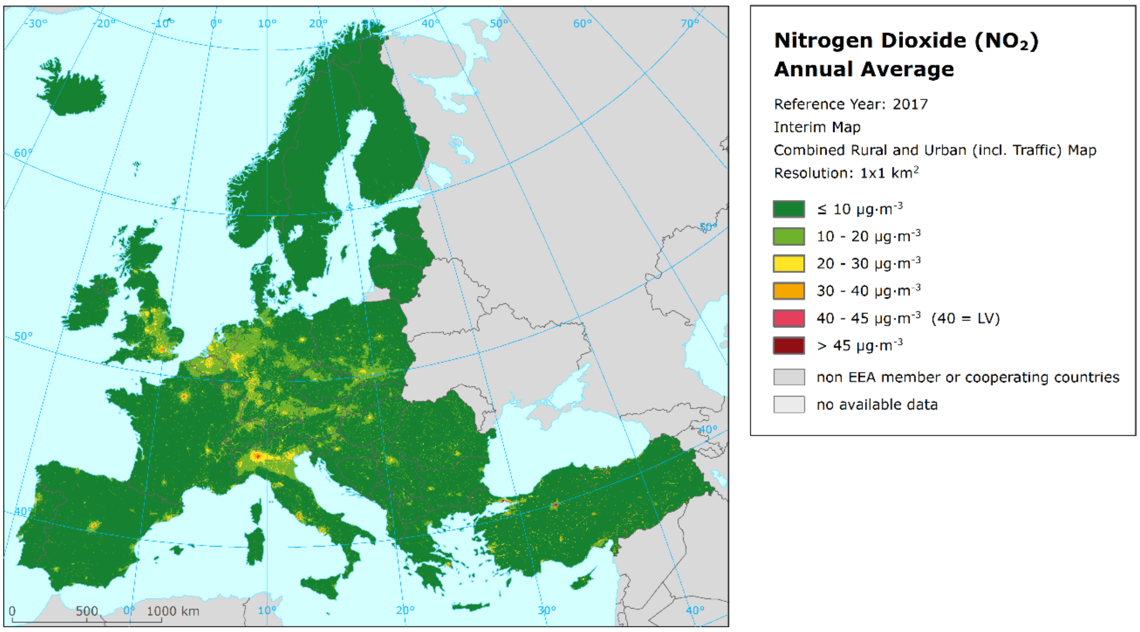

Map 4.4 shows difference maps between the interim map and the reference map (Horálek et al., 2020). The differences are not so distinct as in the case of PM_{10}. The main differences are in the urban areas of Turkey.

Map 4.4 Difference map of NO_2 annual average, 2017, interim map using E2a measurement, pseudo data and CAMS-ENS Forecast model data minus reference map using E1a measurement and EMEP model data

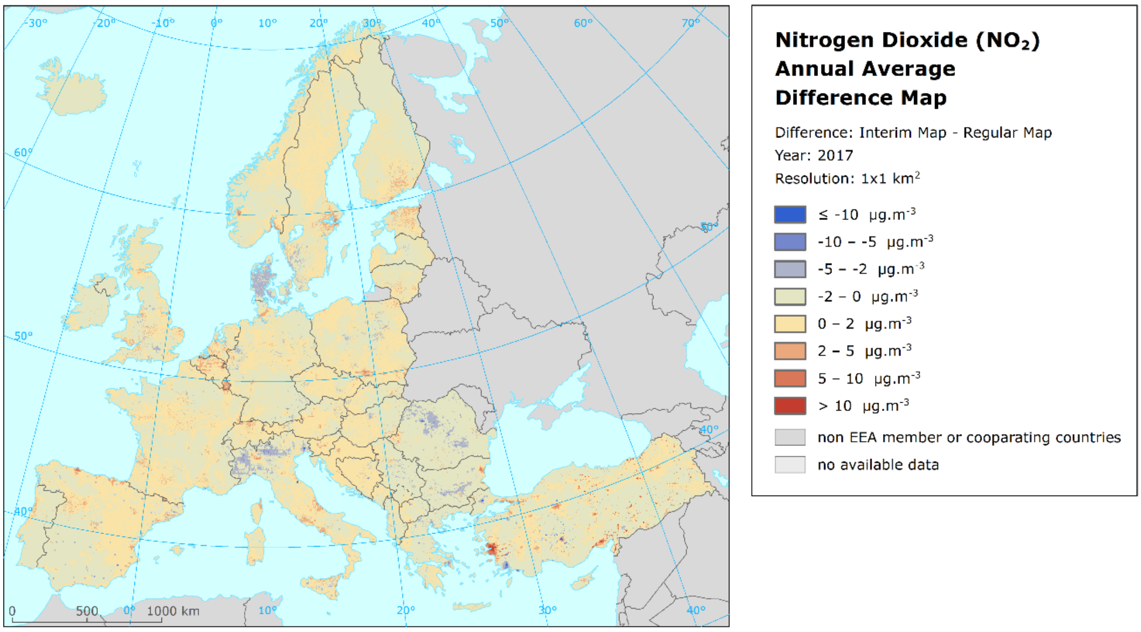

It can be concluded that the interim mapping of NO_2 is possible, apart from the area of Turkey (covered with no E2a data, showing high uncertainty), which is recommended not to map at this stage.

4.3 Ozone – SOMO35

The interim mapping for ozone based on the E2a measurement and CAMS modelling data is examined in this paper for the first time: In contrast to PM_{10} and NO_2, it was not tested in Horálek et al. (2020a).

At first, the pseudo stations data have been estimated, based on the E1a measurement data for 2016, the CAMS Ensemble Forecast modelling data for 2016 and 2017, and the regression relation with the E2a measurement data for 2017. Table 4.9 gives the regression coefficients determined for pseudo stations data estimation, based on the 1133 rural and urban/suburban background stations that have both E1a 2016 and E2a 2017 measurements available (see Section 2.2). Next to this, it presents the statistics showing the tentative quality of the estimate.

Table 4.9 Parameters and statistics of linear regression model for generation of pseudo ozone data in rural and urban background and urban traffic areas, for ozone indicator SOMO35, 2017

Ozone		Rural and urban background areas
Linear regression model (LRM, Eq. 2.4)	c (constant)	330.4
	a1 (O_3 SOMO35 2016, E1a data)	
	a2 (O_3 SOMO35 * CAMS ratio 2017/2016)	0.811
	Adjusted R^2	**0.85**
	Standard Error [μg.m^{-3}]	**835.8**

Table 4.10 shows the validation of the pseudo data, using E1a stations not included in the E2a data set, for different types of area. Again, next to the analysis for the entire mapping area, separate comparison for two distinct areas we have been executed: first, for areas covered by E2a data (i.e., without Italy, Bulgaria, Romania, Serbia, Cyprus and Turkey) and for areas not covered by the E2a data (i.e., for Italy, Bulgaria, Romania, Serbia, Cyprus and Turkey). Like in the case of PM_{10} and NO_2, for urban background areas not covered by the E2a data, we present the results separately for areas outside Turkey and for Turkey.

Table 4.10 Validation of pseudo ozone data showing RMSE, RRMSE, bias, R^2 and linear regression from validation scatter plots for rural background (top) and urban/suburban background stations (bottom), ozone indicator SOMO35, 2017. Validation by E1a stations not used in mapping. Units: μg.m^{-3}.d except RRMSE and R^2.

O_3 – Rural background stations						
Validation set	**Area**	**RMSE**	**RRMSE**	**Bias**	**R^2**	**Regr. eq.**
E1a stations not in E2a data set	Entire area	1805	23.6%	-111	0.757	y = 0.999x - 103
	Area covered by E2a data	1672	30.3%	-335	0.718	y = 0.770x + 933
	Area not covered by E2a data	1860	21.7%	-13	0.724	y = 1.082x - 715
O_3 - Urban/suburban background stations						
Validation set	**Area**	**RMSE**	**RRMSE**	**Bias**	**R^2**	**Regr. eq.**
E1a stations not in E2a data set	Entire area	1854	35.3%	173	0.712	y = 0.925x + 568
	Area covered by E2a data	1146	34.4%	-25	0.762	y = 0.797x + 651
	Area not covered by E2a data, no TR	2006	30.6%	117	0.634	y = 0.987x + 204
	Area not covered by E2a data, TR	2209	105.1%	964	0.472	y = 0.745x + 1500

Note: Areas not covered by E2a data are comprised of IT, BG, RO, RS, CY and TR.

Looking at the validation results, one can see that the ozone pseudo data estimates are poorer, compared to both PM_{10} and NO_2 pseudo data. Apart from the area of Turkey, the R^2 is in between 0.6 and 0.8, while the relative uncertainty RRMSE is in between 20 % and 35 %. Nevertheless, we have further used the pseudo data estimates, due to the reasonable small bias (in between -6 % and 4 % in relative numbers, apart from Turkey).

Based on the E2a data and pseudo data, CAMS Ensemble Forecast modelling data and other supplementary data as used in the regular mapping, the interim map of the ozone indicator SOMO35 for 2017 has been created.

Table 4.11 presents the estimated parameters of the linear regression models (*c, a_1, a_2,…*) and of the residual kriging (*nugget, sill, range*) and includes the statistical indicators of both the regression and the kriging of its residuals.

Table 4.11 Parameters and statistics of linear regression model and ordinary kriging in rural and urban background for interim map of ozone indicator SOMO35 for 2017

Ozone		SOMO35	
		Rural areas	Urban areas
Linear regresion model (LRM, Eq. 2.1)	c (constant)	-229	28702
	a1 (CAMS-ENS-FC model)	0.85	0.56
	a2 (altitude GMTED)	3.28	
	a3 (wind speed)		-218.07
	a4 (s. solar radiation)	*n. sign.*	
	a5 (relative humidity)		-2.854
	Adjusted R^2	**0.63**	**0.56**
	Standard Error [$\mu g.m^{-3}.d$]	**1693**	**1527**
Ord. krig. (OK) of LRM residuals	nugget	2.2E+06	8.0E+05
	sill	2.4E+06	1.6E+06
	range [km]	670	70
LRM + OK of its residuals	**RMSE [$\mu g.m^{-3}$.days]**	**1285**	**1054**
	Relative RMSE [%]	**27.3%**	**26.9%**
	Bias (MPE) [$\mu g.m^{-3}.d$]	**1**	**-1**

Table 4.12 presents the evaluation of the interim map, based on the E1a station data not included in the E2a data set, for different areas types.

Table 4.12 Validation of interim RIMM spatial mapping showing RMSE, RRMSE, bias, R^2 and linear regression from validation scatter plots for ozone indicator SOMO35 for 2017 in rural background (top) and urban background (bottom). Cross-validation and validation by E1a stations not used in mapping. Units: $\mu g.m^{-3}$ except RRMSE and R^2.

O_3 – Rural background areas								
Validation set	**Area**	**Type of valid.**	**Type of map**	**RMSE**	**RRMSE**	**Bias**	**R^2**	**Regr. eq.**
E1a stations in E2a set	Area covered by E2a data	Cross-validation	Rural map layer	1285	27.4%	1	0.720	y = 0.737x + 1269
E1a stations not in E2a data set	Entire area	Simple grid validation	Rural map layer	2228	30.7%	-641	0.593	y = 0.492x + 3044
			Final merged map	2299	31.7%	-829	0.581	y = 0.509x + 2736
	Area covered by E2a data	Simple grid validation	Rural map layer	1432	27.8%	-242	0.781	y = 0.659x + 1515
			Final merged map	1545	30.0%	-345	0.738	y = 0.659x + 1414
	Area not covered by E2a data	Simple grid validation	Rural map layer	2549	30.5%	-851	0.325	y = 0.272x + 5234
			Final merged map	2609	31.2%	-1084	0.333	y = 0.321x + 4591

O_3 – Urban background areas								
Validation set	**Area**	**Type of valid.**	**Type of map**	**RMSE**	**RRMSE**	**Bias**	**R^2**	**Regr. eq.**
E1a stations in E2a set	Area covered by E2a data	Cross-validation	Urban b. map layer	1008	25.9%	11	0.741	y = 0.756x + 962
E1a stations not in E2a data set	Entire area	Simple grid validation	Urban b. map layer	1927	37.3%	-518	0.653	y = 0.556x + 1775
			Final merged map	1911	37.0%	-325	0.635	y = 0.567x + 1911
	Area covered by E2a data	Simple grid validation	Urban b. map layer	1132	33.5%	-51	0.777	y = 0.619x + 1239
			Final merged map	1063	31.4%	34	0.801	y = 0.656x + 1199
	Area not covered by E2a data, no TR	Simple grid validation	Urban b. map layer	2141	33.3%	-935	0.517	y = 0.511x + 2205
			Final merged map	2138	33.3%	-675	0.464	y = 0.488x + 2613
	Area not covered by E2a data, TR	Simple grid validation	Urban b. map layer	2160	113.5%	880	0.235	y = 0.280x + 2350
			Final merged map	2155	112.3%	948	0.274	y = 0.319x + 2339

Note: Areas not covered by E2a data are comprised of IT, BG, RO, RS, CY and TR.

Examining the validation statistics, one can see somewhat poorer results compared to both PM_{10} and NO_2. Specifically, the areas not covered by the E2a data show the underestimation of the final map of almost 1100 $\mu g.m^{-3}\cdot d$ in the rural areas and 900 $\mu g.m^{-3}\cdot d$ in the urban areas apart from Turkey, what is -13 % and -11 % in relative numbers. The urban area of Turkey again show the highest uncertainty.

Map 4.5 presents the final merged interim map of the ozone indicator SOMO35 for 2017.

Map 4.5 Interim concentration map of ozone indicator SOMO35, 2017, RIMM methodology using E2a (UTD) measurement data, pseudo data and CAMS-ENS Forecast model output

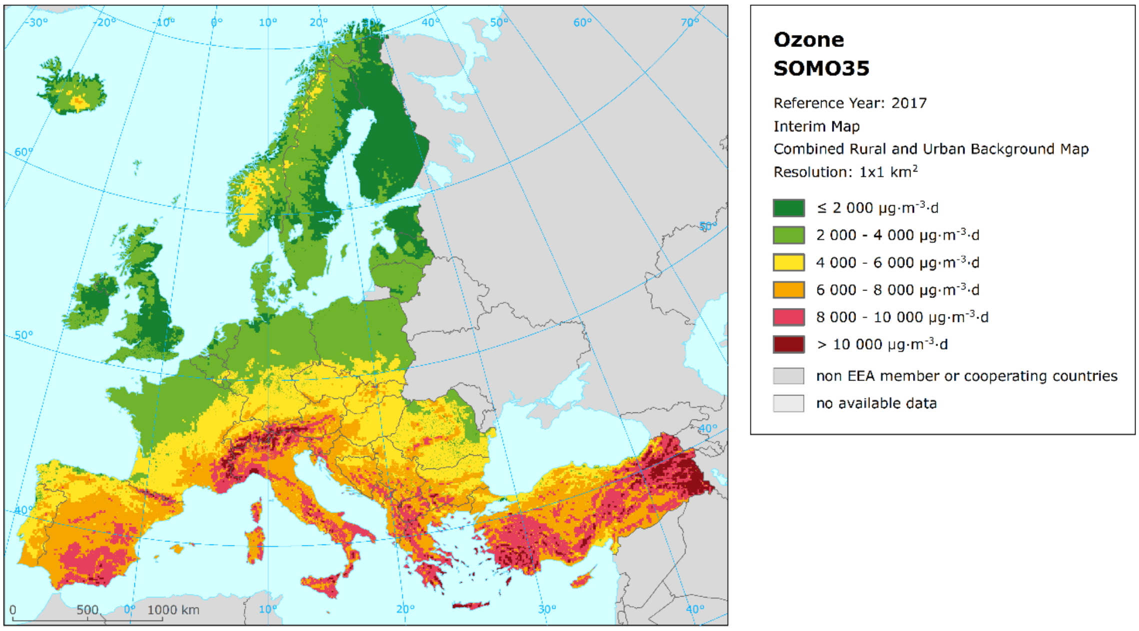

Map 4.6 shows difference maps between the interim map and the reference map (Horálek et al., 2020). It can be seen that the differences take place especially in areas with a low coverage of the E2a data (Turkey, Balkan, Italy, Scandinavia). Differences in Scandinavia are caused by differences in EMEP and CAMS-ENS Forecast models together with a different relation with altitude in the linear regression model, while the differences in Italy, Balkan and Turkey are caused by the bias of the pseudo stations.

It can be concluded that the interim mapping is possible in areas covered by the E2a data. The area of Turkey should not be mapped in the current stage of the E2a (UTD) data coverage. Concerning other areas poorly covered by the E2a data, the current interim mapping leads into a bias, in average to the underestimation of cc 10-15 %, both in the rural and the urban background areas. Further examination is recommended, together with a checking of the actual E2a data coverage.

Map 4.6 Difference map of ozone indicator SOMO35, 2017, interim map using E2a measurement, pseudo data and CAMS-ENS Forecast model data minus reference map using E1a measurement and EMEP model data

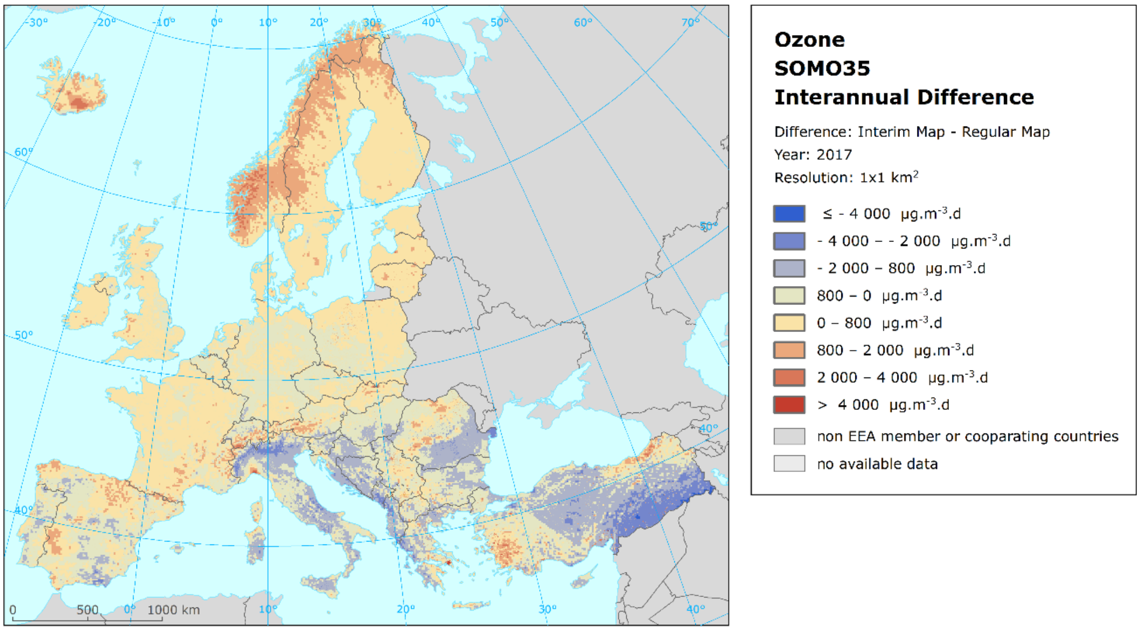

4.4 $PM_{2.5}$ Annual Average

We have briefly checked the possibility to prepare the interim map for $PM_{2.5}$. However, we have faced a limitation of a low number of the stations with the E2a data, specifically in the rural areas. For the numbers of the stations, see Table 3.2. Next to this, these stations are distributed irregularly, with considerable gaps in large parts of Europe. Map 4.7 shows the rural and urban/suburban background stations with the E2a data available. Note that potential pseudo station estimates would have to be derived out of these stations, which would lead to considerable uncertainties.

Due to the low number of the E2a data, we have decided not to perform this mapping for this year.

Map 4.7 Spatial distribution of $PM_{2.5}$ background stations to be potentially used in mapping, 2017

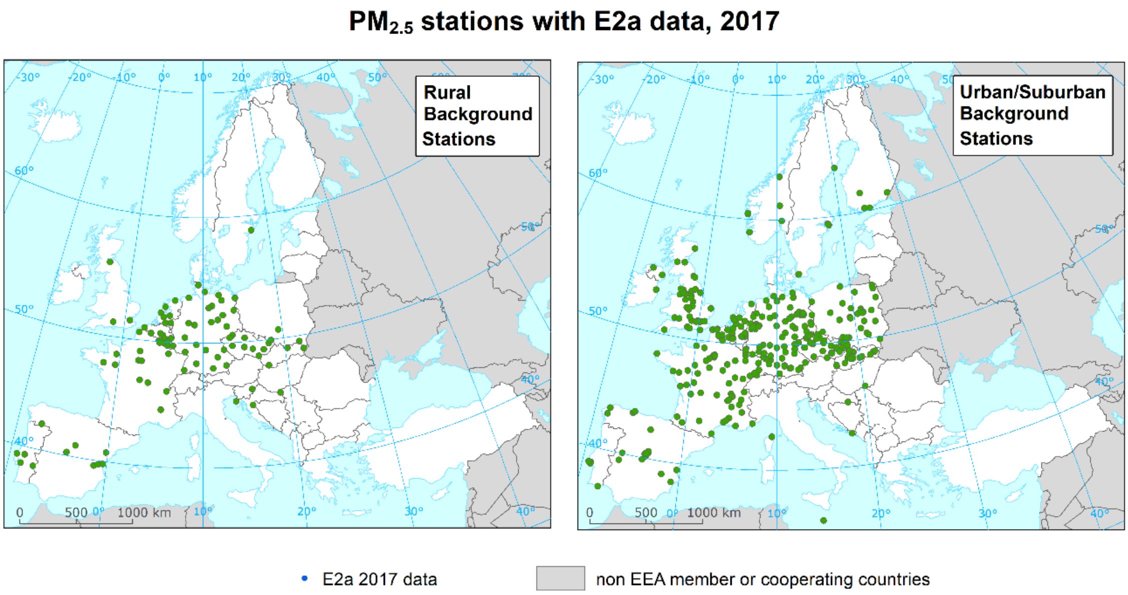

5 Interim Air Quality Spatial Maps for 2019

In this chapter, we present the interim maps 2019, created primarily based on the E2a measurement data for 2019 and the CAMS-Ensemble Forecast modelling data for 2019. Contrary to the maps for 2017 as presented in Chapter 4, no validation based on the validated E1a measurement data has been performed, as the E1a data for 2019 were not available in the time designated for this study.

5.1 PM_{10} Annual Average

Like for 2017, the pseudo stations data have been estimated at first. The estimates have been calculated based on the E1a measurement data for 2018, the CAMS Ensemble Forecast modelling data for 2018 and 2019, and the regression relation with the E2a measurement data for 2019. Table 5.1 presents the regression coefficients determined for pseudo stations data estimation, based on the 1034 rural and urban/suburban background and 471 urban/suburban traffic stations that have both E1a 2018 and E2a 2019 measurements available (see Section 3.1). Next to this, it presents the statistics showing the tentative quality of the estimate.

Table 5.1 Parameters and statistics of linear regression model for generation of pseudo PM_{10} data in rural and urban background and urban traffic areas, for PM_{10} annual average 2019

PM_{10}		Rural and urban background areas	Urban traffic areas
Linear regression model (LRM, Eq. 2.4)	c (constant)	1.3	2.0
	a1 (PM_{10} annual mean 2018, E1a data)	0.179	0.431
	a2 (PM_{10} annual mean 2018 * CAMS ratio 2019/2018)	0.712	0.413
	Adjusted R^2	**0.89**	**0.88**
	Standard Error [μg.m^{-3}]	**2.1**	**2.2**

Based on the E2a data and pseudo data, CAMS Ensemble Forecast modelling data and other supplementary data as used in the regular mapping, the interim PM_{10} annual average map for 2019 has been created. Table 5.2 presents the estimated parameters of the linear regression models (*c, a_1, a_2,…*) and of the residual kriging (*nugget, sill, range*) and includes the statistical indicators of both the regression and the kriging of its residuals.

Table 5.2 Parameters and statistics of linear regression model and ordinary kriging in rural, urban background and urban traffic areas for interim map of PM_{10} annual average 2019

PM_{10}		Annual average		
		Rural areas	Urban b. areas	Urban tr.. areas
Linear regresion model (LRM, Eq. 2.1)	c (constant)	1.66	0.89	1.74
	a1 (log. CAMS-ENS FC model)	0.727	0.86	0.587
	a2 (altitude GMTED)	-0.00024		
	a3 (relative humidity)	-0.00059		
	a4 (wind speed)	-0.656		-0.042
	a5 (land cover NAT1)	-0.0015		
	Adjusted R^2	**0.63**	**0.39**	**0.46**
	Standard Error [μg.m^{-3}]	**0.23**	**0.31**	**0.23**
Ordinary kriging (OK) of LRM residuals	nugget	0.022	0.017	0.013
	sill	0.045	0.053	0.032
	range [km]	620	270	360
LRM + OK of its residuals	**RMSE [μg.m^{-3}]**	**2.7**	**3.4**	**3.7**
	Relative RMSE [%]	**18.6**	**17.3**	**17.5**
	Bias (MPE) [μg.m^{-3}]	**0.0**	**0.0**	**-0.3**
	R^2 of cross.-val. regr. equation	**0.73**	**0.70**	**0.67**
	Slope of cross-val. regr. equation	**0.72**	**0.76**	**0.68**
	Intercept of cross-val. regr. equation	**4.2**	**4.7**	**6.5**

Map 5.1 presents the final merged interim map of the PM_{10} annual average for 2019.

Map 5.1 Interim concentration map of PM_{10} annual average, 2019, RIMM methodology using E2a (UTD) measurement data, pseudo data and CAMS-ENS Forecast model output

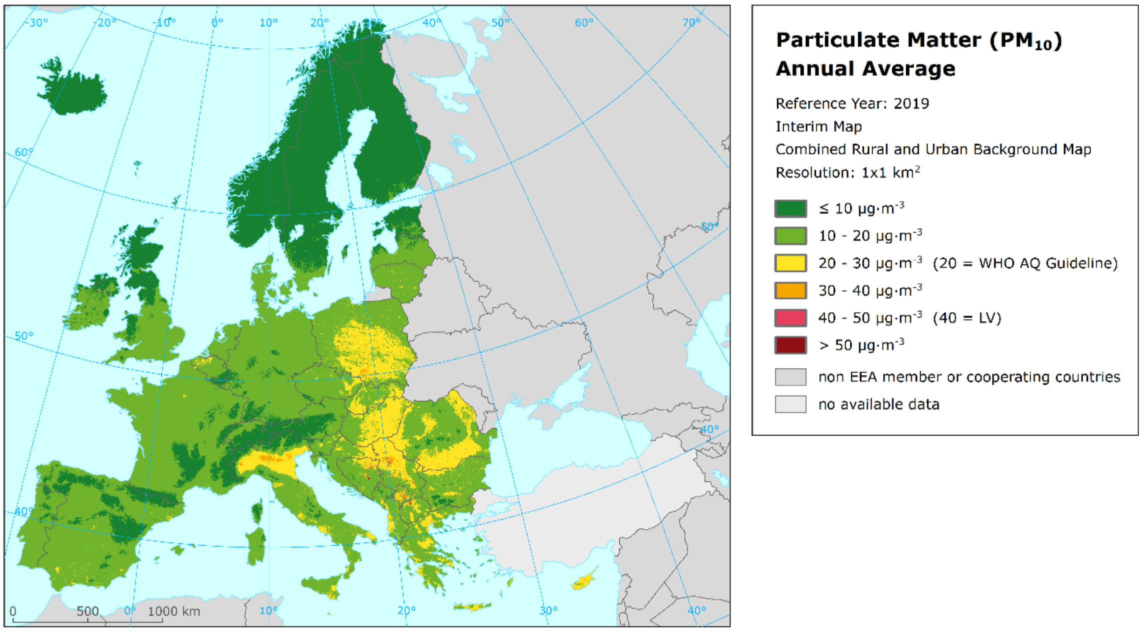

5.2 NO_2 Annual Average

As a first step for the interim NO_2 annual average 2019 map creation, the pseudo stations data have been estimated, based on the E1a measurement data for 2018, the CAMS Ensemble Forecast modelling data for 2018 and 2019, and the regression relation with the E2a measurement 2019 data. Table 5.3 presents the regression coefficients determined for pseudo stations data estimation, based on the 1361 rural and urban/suburban background and 634 urban/suburban traffic stations that have both E1a 2018 and E2a 2019 measurements available (see Section 3.1). Apart from this, it gives the statistics showing the tentative quality of the estimate.

Table 5.3 Parameters and statistics of linear regression model for generation of pseudo NO_2 data in rural and urban background and urban traffic areas, for NO_2 annual average 2019

NO_2		**Rural and urban background areas**	**Urban traffic areas**
Linear regression model (LRM, Eq. 2.4)	c (constant)	-0.1	1.8
	a1 (NO_2 annual mean 2018, E1a data)	0.868	0.866
	a2 (NO_2 annual mean 2018 * CAMS ratio 2019/2018)	0.086	*n. sign.*
	Adjusted R^2	**0.95**	**0.91**
	Standard Error [µg.m^{-3}]	**1.6**	**3.1**

Based on the E2a data and pseudo data, CAMS Ensemble Forecast modelling data and other supplementary data as used in the regular mapping, the interim NO_2 annual average map for 2019 has been created. Compared to the 2017 maps, for 2019, Sentinel-5P satellite data have been used instead of the OMI satellite data, in agreement with the development in the regular mapping.

Table 5.4 presents the estimated parameters of the linear regression models (*c, a_1, a_2,…*) and of the residual kriging (*nugget, sill, range*) and includes the statistical indicators of both the regression and the kriging of its residuals.

Table 5.4 Parameters and statistics of linear regression model and ordinary kriging in rural, urban background and urban traffic areas for interim map of NO_2 annual average 2019

NO_2		Annual average		
		Rural areas	**Urb. b. areas**	**Urb. tr. areas**
Linear regesion model (LRM, Eq. 2.1)	c (constant)	4.6	15.9	23.00
	a1 (CAMS-ENS-FC model)	0.582	0.192	*n.sign.*
	a6 (satellite Sentinel-5P)	0.91	1.593	2.035
	a2 (altitude)	-0.0071	*n.sign.*	*n.sign.*
	a3 (altitude_5km_radius)	0.0067	*n.sign.*	*n.sign.*
	a4 (wind speed)	-0.64	-1.964	-1.631
	a7 (population*1000)	0.00157	0.00021	
	a8 (NAT_1km)		-0.0535	
	a9 (AGR_1km)		-0.0452	
	a10 (TRAF_1km)		0.0640	
	a11 (LDR_5km_radius)	*n.sign.*	*n.sign.*	0.1407
	a12 (HDR_5km_radius)		0.0905	0.3011
	a13 (NAT_5km_radius)	-0.0250		
	Adjusted R^2	**0.77**	**0.52**	**0.38**
	Standard Error [μg.m^{-3}]	**2.4**	**5.2**	**8.5**
Ordinary kriging (OK) of LRM residuals	nugget	2	13	35
	sill	2	18	832
	range [km]	14	90	130
LRM + OK of its residuals	**RMSE [μg.m^{-3}]**	**2.2**	**4.0**	**7.4**
	Relative RMSE [%]	**27.7**	**22.7**	**25.5**
	Bias (MPE) [μg.m^{-3}]	**-0.1**	**0.0**	**0.2**
	R^2 of cross-val. regr. equation	**0.79**	**0.64**	**0.50**
	Slope of cross-val. regr. equation	**0.79**	**0.66**	**0.54**
	Intercept of cross-val. regr. equation	**1.5**	**5.9**	**13.4**

Map 5.2 presents the final merged interim map of the NO_2 annual average for 2019.

Map 5.2 Interim concentration map of NO_2 annual average, 2019, RIMM methodology using E2a (UTD) measurement data, pseudo data and CAMS-ENS Forecast model output

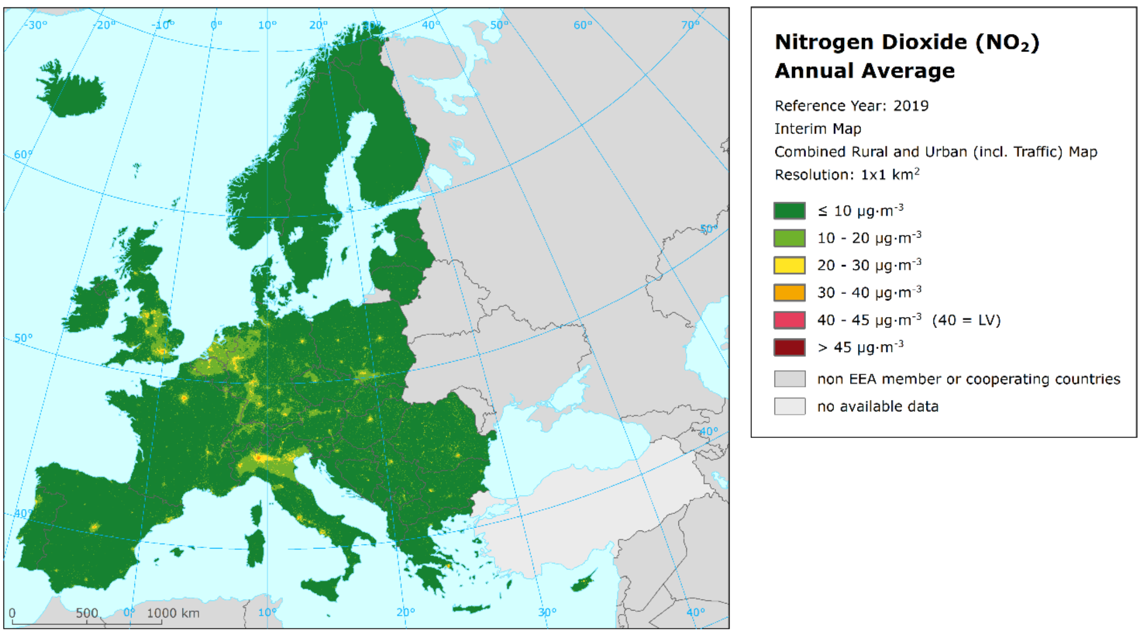

5.3 Ozone – SOMO35

At first, the pseudo stations data have been estimated, based on the E1a measurement data for 2018, the CAMS Ensemble Forecast modelling data for 2018 and 2019, and the regression relation with the E2a measurement data for 2019. Table 5.5 gives the regression coefficients determined for pseudo stations data estimation, based on the 1303 rural and urban/suburban background stations that have both E1a 2018 and E2a 2019 measurements available (see Section 3.1). Next to this, it presents the statistics showing the tentative quality of the estimate. Be it noted that the R^2 of 0.77 means quite a poor relation (it is the weakest regression relation of the pseudo data estimates in this paper).

Table 5.5 Parameters and statistics of linear regression model for generation of pseudo ozone data in rural and urban background and urban traffic areas, for ozone indicator SOMO35, 2019

Ozone		Rural and urban background areas
Linear regression model (LRM, Eq. 2.4)	c (constant)	21.7
	a1 (O_3 SOMO35 2018, E1a data)	0.314
	a2 (O3 SOMO35 * CAMS ratio 2019/2018)	0.591
	Adjusted R^2	**0.77**
	Standard Error [μg.m^{-3}]	**1046.4**

Based on the E2a data and pseudo data, CAMS Ensemble Forecast modelling data and other supplementary data as used in the regular mapping, the interim map of the ozone indicator SOMO35 for 2019 has been created. Due to the increasing data coverage of the E2a data and the weak estimate of the pseudo data, we have additionally prepared also the SOMO35 interim map for 2019 based on the E2a data (and supplementary data) only, without the use of the pseudo data.

Table 5.6 presents the estimated parameters of the linear regression models (*c, a_1, a_2,…*) and of the residual kriging (*nugget, sill, range*) and includes the statistical indicators of both the regression and the kriging of its residuals, for both map variants.

Table 5.6 Parameters and statistics of linear regression model and ordinary kriging in rural and urban background areas for interim map of ozone indicator SOMO35 for 2019

Ozone		SOMO35			
		Using pseudo stations		Without pseudo stations	
		Rural areas	Urban areas	Rural areas	Urban areas
Linear regresion model (LRM, Eq. 2.1)	c (constant)	1034	2734	21	2494
	a1 (CAMS-ENS-FC model)	0.76	0.62	1.01	0.81
	a2 (altitude GMTED)	2.79		3.08	
	a3 (wind speed)		-415.2		-548.7
	a4 (s. solar radiation)	*n. sign.*	*n.sign.*	*n. sign.*	*n.sign.*
	Adjusted R^2	**0.43**	**0.29**	**0.64**	**0.49**
	Standard Error [μg.m^{-3}.d]	**1894**	**1878**	**1418**	**1441**
Ord. krig. (OK) of LRM residuals	nugget	1.7E+06	1.4E+06	1.4E+06	8.2E+05
	sill	1.2E+06	6.9E+05	4.7E+05	4.9E+05
	range [km]	190	290	420	230
LRM + OK of its residuals	**RMSE [μg.m^{-3}.days]**	**1481**	**1209**	**1344**	**1173**
	Relative RMSE [%]	**25.4**	**25.1**	**23.1**	**24.4**
	Bias (MPE) [μg.m^{-3}.d]	**-95**	**-63**	**8**	**8**
	R^2 of cross.-val. regr. equation	**0.61**	**0.63**	**0.68**	**0.65**
	Slope of cross-val. regr. equation	**0.58**	**0.60**	**0.67**	**0.66**
	Intercept of cross-val. regr. equation	**2336**	**1900**	**1911**	**1662**

Contrary to the interim mapping for 2017 as presented in Chapter 4, neither the validation based on the validated E1a measurement nor the comparison with the regular 2019 map has been done. Thus, we cannot evaluate the quality of the map in the areas outside the E2a data. Concerning the areas covered by the E2a data, by comparing the cross-validation results as presented in Table 5.6, one can state that the variant without the use of the pseudo data gives slightly better results. However, we can suppose that in the areas not covered by the E2a data, the variant using the pseudo data estimates might give better results. Thus, we present this variant as a basic one. Map 5.3 presents the final merged interim map of the ozone indicator SOMO35 for 2019 (in the variant using the pseudo data).

Map 5.3 Interim concentration map of ozone indicator SOMO35, 2019, RIMM methodology using E2a (UTD) measurement data, pseudo data and CAMS-ENS Forecast model output

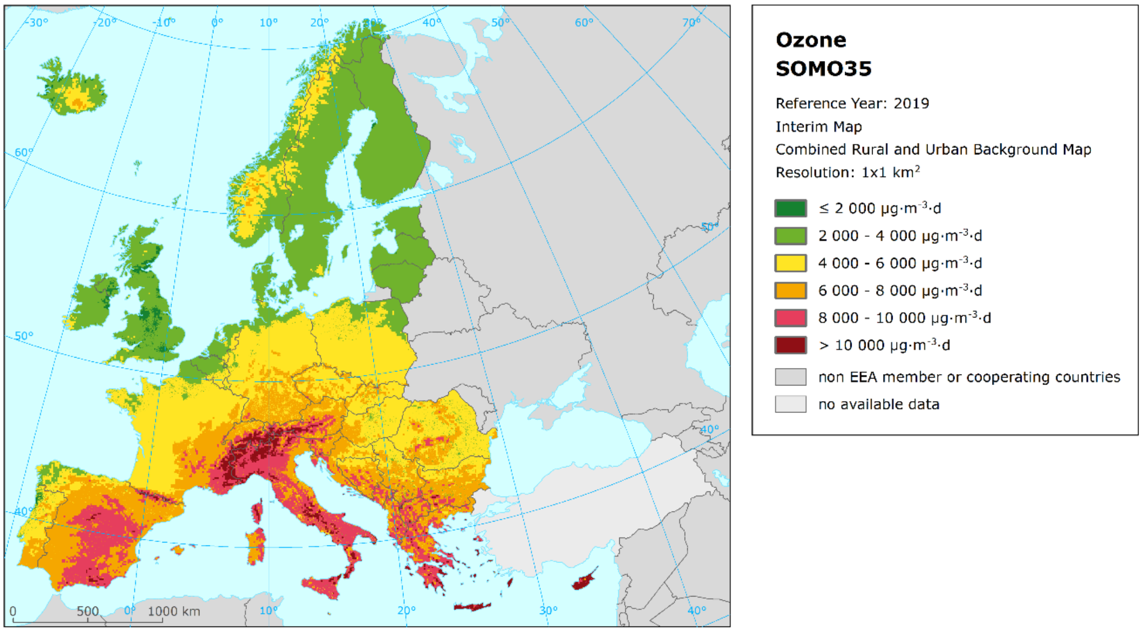

Map 5.4 presents the difference between the interim map using the pseudo data (as presented in Map 5.3) and the interim map without the use of the pseudo data.

Map 5.4 Difference map of ozone indicator SOMO35, 2019, interim map using pseudo data together with the E2a measurement and CAMS-ENS Forecast model data minus interim map using the E2a measurement and CAMS-ENS Forecast model data without the pseudo data

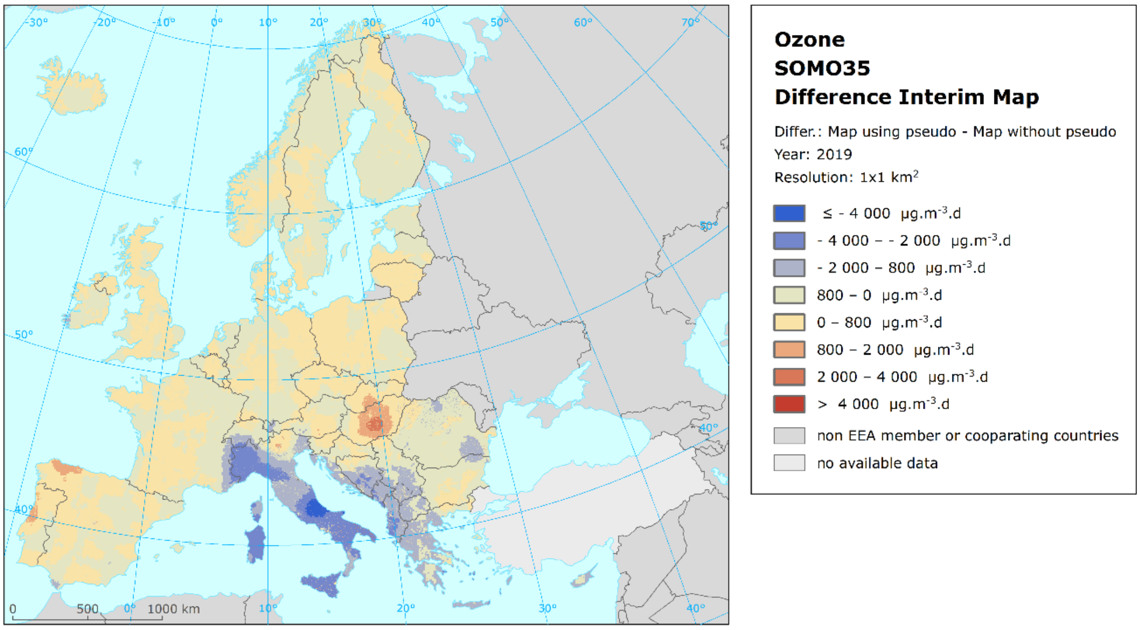

One can see the differences only in areas with a poor coverage of the E2a data (Italy, Balkan). In agreement with the results presented in Section 4.3 (and particularly in Table 4.12), one can suppose that the areas not covered by the E2a data might be somewhat underestimated. This leads into the recommendation that in future, when the data coverage of the E2a data is larger, interim ozone maps can be constructed without the use of the pseudo stations. However, such interim maps should be tested against the validated data, when available.

6 Conclusions and Recommendations

The report examines the creation of interim air quality annual maps.

The production of interim AQ mapping based on interim E2a data and the CAMS ensemble regional forecast modelling data appears to be feasible and the resulting interim AQ maps have proven to have adequate skill for PM_{10} annual average, NO_2 annual average and ozone indicator SOMO35. We therefore conclude that these mapping products have utility as a product for the evaluation of European AQ at an earlier juncture than would be otherwise possible using the combination of EMEP model and E1 data alone. Indeed, we estimate that these interim mapping products could be produced and made available as early as the end of April in the year subsequent to the analysis year, i.e. one year earlier compared to the regular maps based on the official reported E1a data. In terms of skill, the interim AQ maps give satisfactory performance, in general.

There are some notable limitations of these AQ mapping products, however. First, it should be stated clearly that since the interim maps are based on un-validated data the maps should not be considered definitive. Indeed, while the interim AQ maps have an adequate performance in general, the statistical evaluation against E1a data shows a bias (i.e., somewhat lower results) for ozone in the areas poorly covered by the E2a data. Their utility, therefore, is strictly for guidance purposes in support of annual reporting of AQ by member states. In addition, the absence of any E2a data from Turkey and a high uncertainty of the mapping results in the relevant area severely limits the utility of the interim maps over this country.

Next to Turkey, the E2a data gaps threaten the interim mapping also in some other areas. In order to overcome this obstacle, we have examined the use of so-called pseudo stations data in the interim mapping. The estimates of these pseudo stations data are based on the regression relation between the E2a data from the year Y and the validated E1a data from the year Y-1, together with the ratio of the modelling results from years Y and Y-1. The pseudo station estimates give good results for PM_{10} and NO_2, while somewhat poorer results for ozone. For ozone, their use in the interim mapping leads into the underestimation of ca. 10-15 % in areas not covered by the E2a data. The use of the pseudo station data in the interim mapping is recommended for PM_{10} and NO_2. For ozone, the potential use of the pseudo data should be provisional only, until the data coverage of the E2a data is larger and the interim ozone maps might be constructed without the use of the pseudo stations. The construction of the ozone interim maps is a subject for improvement and the performance of these maps should be tested against the validated data, when available.

We have also briefly checked the possibility to prepare the interim map for $PM_{2.5}$, but due to a low number of the E2a data and their irregular spatial distribution (specifically in the rural areas), we have decided not to perform the interim mapping for this pollutant. In future, we might reconsider this, when more E2a data for $PM_{2.5}$ is available.

Due to the key advantage of the interim maps (i.e., timeliness) and their sufficient quality we recommend that the production of interim AQ maps (for basic PM_{10}, NO_2 and ozone indicators) based on CAMS regional ensemble forecast and E2a data become part of the routine AQ mapping carried out by ETC/ATNI, next to the regular maps created based on the validated E1a data. We believe the increased timeliness of delivery will greatly support annual reporting of AQ by member states.

It should be noted that only the spatial maps, but not the exposure estimates have been examined in this report. One should bear in mind that the exposure estimates are more sensible on a bias than the concentration maps. For future, it might be recommended to examine the exposure estimates of the interim maps.

References

Cressie, N., 1993, *Statistics for spatial data,* Wiley series, New York.

Danielson, J. J. and Gesch, D. B., 2011, *Global multi-resolution terrain elevation data 2010 (GMTED2010)*, U.S. Geological Survey Open-File Report, pp. 2011-1073 (https://pubs.er.usgs.gov/publication/ofr20111073) accessed 19 November 2020.

EC, 2008, *Directive 2008/50/EC of the European Parliament and of the Council of 21 May 2008 on ambient air quality and cleaner air for Europe,* OJ L 152, 11.06.2008, 1-44 (http://eur-lex.europa.eu/LexUriServ/LexUriServ.do?uri=OJ:L:2008:152:0001:0044:EN:PDF) accessed 26 August 2020.

EEA, 2016, *Corine land cover 2012 (CLC2012) raster data*, 100x100 m^2 gridded version 18 (09/2016 (https://sdi.eea.europa.eu/catalogue/srv/api/records/ff21ade0-a714-4725-86bb-279ee7a8a73e) accessed 10 January 2020.

EEA, 2020, *Air Quality e-Reporting. Air quality database (*https://www.eea.europa.eu/data-and-maps/data/aqereporting-8). Data extracted in March 2020.

EU, 2020, *Corine land cover 2018 (CLC2018) raster data*, 100x100m^2 gridded version 2020_20 (https://land.copernicus.eu/pan-european/corine-land-cover/clc2018) accessed 19 November 2020.

Eurostat, 2014, *GEOSTAT 2011 grid dataset. Population distribution dataset* (http://ec.europa.eu/eurostat/web/gisco/geodata/reference-data/population-distribution-demography) accessed 26 August 2020.

Horálek, J., et al., 2014, *Evaluation of Copernicus MACC-II ensemble products in the ETC/ACM spatial air quality mapping,* ETC/ACM Technical Paper 2013/9 (http://www.eionet.europa.eu/etcs/etc-atni/products/etc-atni-reports/etcacm_tp_2013_9_aqmaps_with_maccproducts) accessed 15 June 2021.

Horálek, J., et al., 2020, *European air quality maps for 2017*, Eionet Report ETC/ATNI 2019/9, (https://doi.org/10.5281/zenodo.4309292) accessed 8 December 2020.

Horálek, J., et al., 2021a, *Potential use of CAMS modelling results in air quality mapping under ETC/ATNI*, Eionet Report ETC/ATNI 2019/17, (https://doi.org/10.5281/zenodo.4627762) accessed 15 June 2021.

Horálek, J., et. al., 2021b, *European air quality maps for 2018*, Eionet Report ETC/ATNI 2020/10 (https://doi.org/10.5281/zenodo.4638651) accessed 15 June 2021.

Kuenen, J. J. P., et al., 2014, 'TNO-MACC_II emission inventory; a multi-year (2003--2009) consistent high-resolution European emission inventory for air quality modelling', *Atmospheric Chemistry and Physics*, 14, pp. 10963–10976 (https://doi.org/10.5194/acp-14-10963-2014) accesed 16 February 2021.

Marécal, V., et al., 2015, 'A regional air quality forecasting system over Europe: The MACC-II daily ensemble production', *Geoscientific Model Development*, 8, pp. 2777–2813 (https://doi.org/10.5194/gmd-8-2777-2015) accesed 16 February 2021.

Meijer, J. R., et al., 2018, 'Global patterns of current and future road infrastructure', *Environmental Research Letters*, 13 0640, (https://doi.org/10.1088/1748-9326/aabd42) accesed 10 June 2019.

NASA, 2020, *OMNO2d level 3 satellite data* (https://acdisc.gsfc.nasa.gov/opendap/HDF-EOS5/Aura_OMI_Level3/OMNO2d.003) accessed 26 March 2020.

NILU, 2020, *EBAS, database of atmospheric chemical composition and physical properties* (http://ebas.nilu.no) accessed 26 March 2020.

van Geffen, J., et al., 2020, 'S5P TROPOMI NO2 slant column retrieval: Method, stability, uncertainties and comparisons with OMI', *Atmospheric Measurement Techniques*, 13, pp. 1315–1335 (https://doi.org/10.5194/amt-13-1315-2020) accessed 17 June 2021.

Annex
Maps of measurement stations used for mapping

This Annex presents the maps showing the air quality stations used for the mapping and validation of 2017 interim maps and for the mapping of 2019 interim maps, for three pollutants PM_{10}, NO_2 and ozone.

Maps A.1, A.2 and A.3 show the spatial distribution of the rural, urban/suburban background and urban/suburban traffic stations (for PM_{10} and NO_2) used in the interim 2017 mapping (in green and orange) and validation (in red), for different pollutants. In all figures, the true stations (in green) and the pseudo stations (in orange) are distinguished.

Maps A.4, A.5 and A.6 show the spatial distribution of the rural, urban/suburban background and urban/suburban traffic stations (for PM_{10} and NO_2) used in the interim 2019 mapping, for different pollutants. In all figures, the true stations (in green) and the pseudo stations (in orange) are distinguished.

Map A.1 Spatial distribution of PM_{10} stations used in mapping and validation, 2017

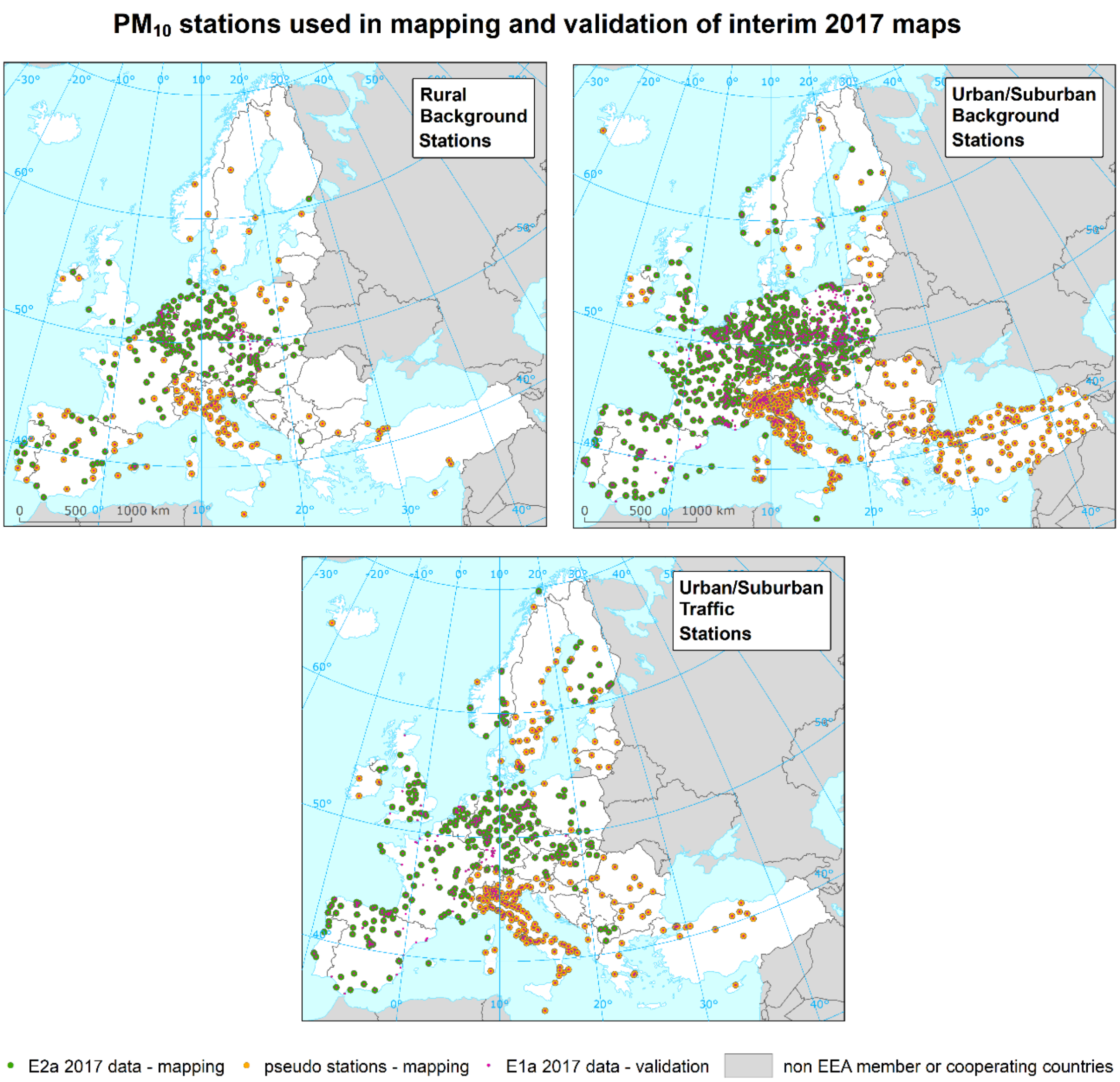

Map A.2 Spatial distribution of NO_2 stations used in mapping and validation, 2017

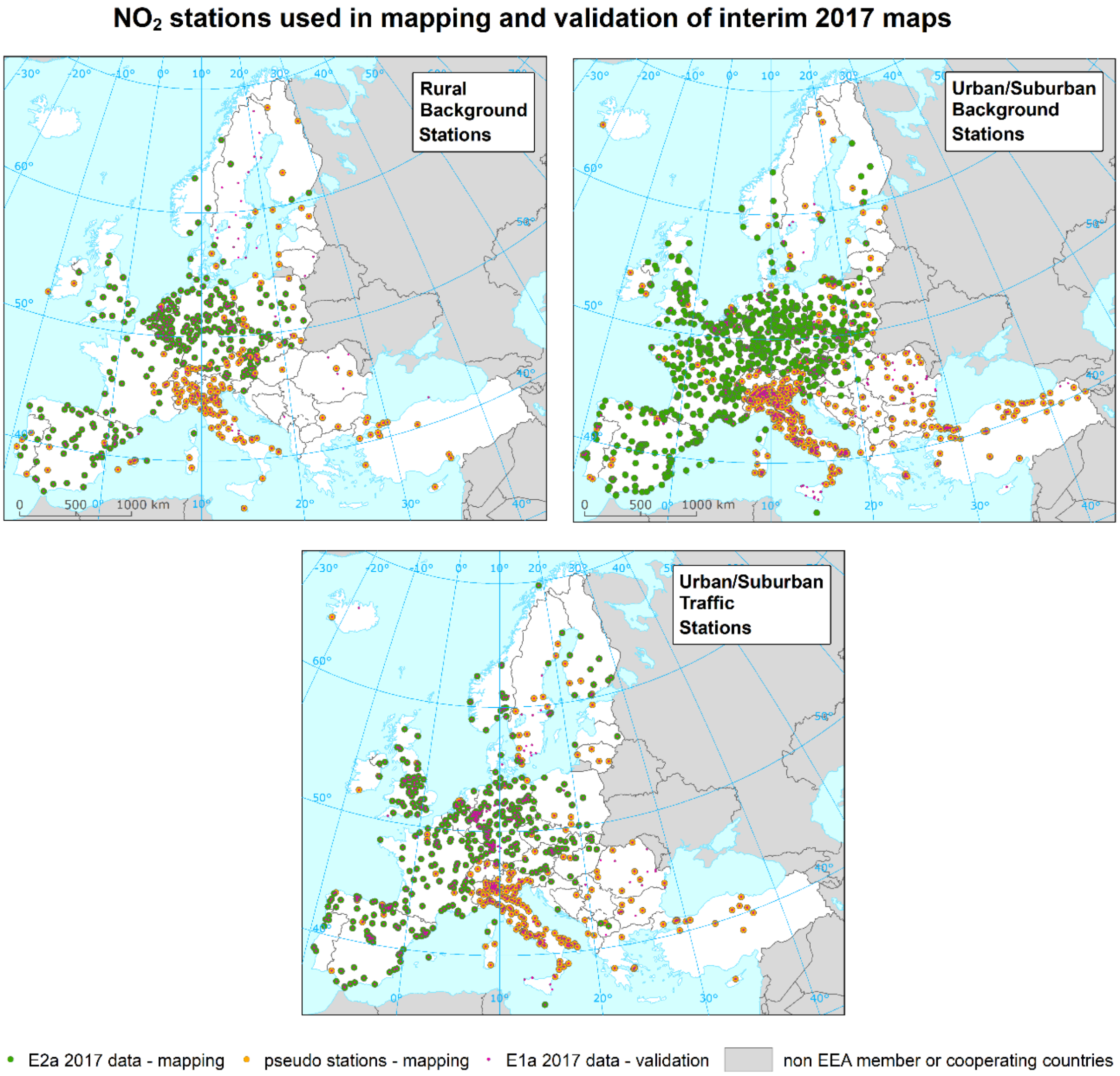

Map A.3 Spatial distribution of O_3 background stations used in mapping and validation, 2017

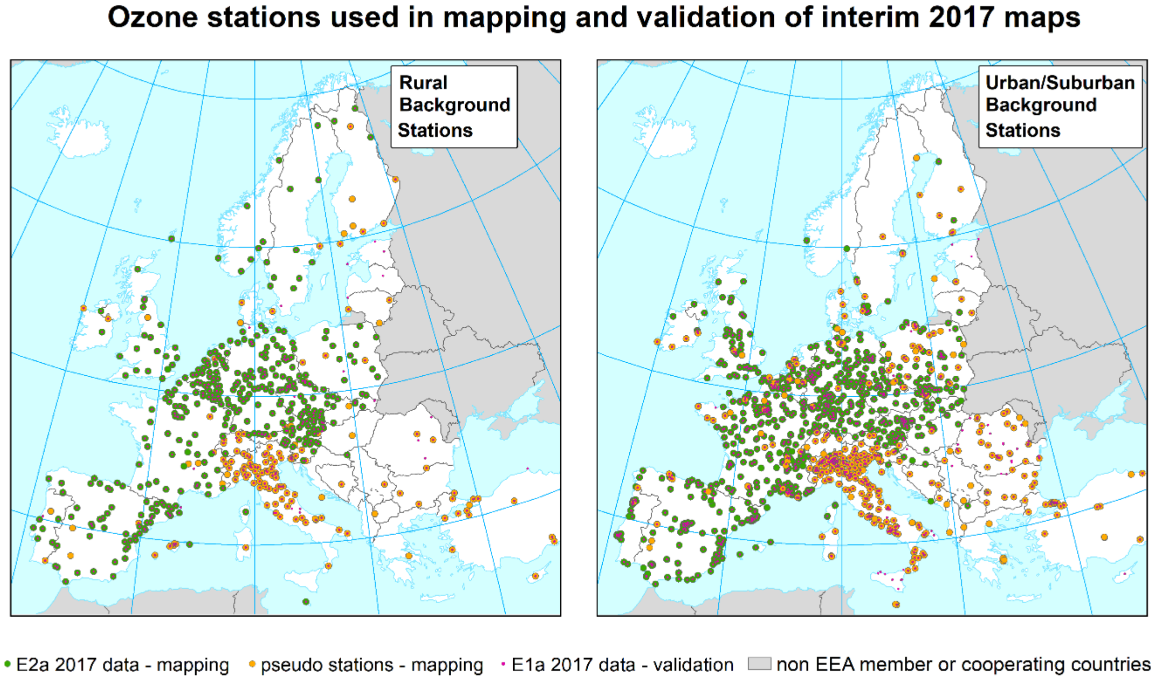

Map A.4 Spatial distribution of PM_{10} stations used in interim mapping, 2019

PM_{10} stations used in mapping of interim 2019 maps

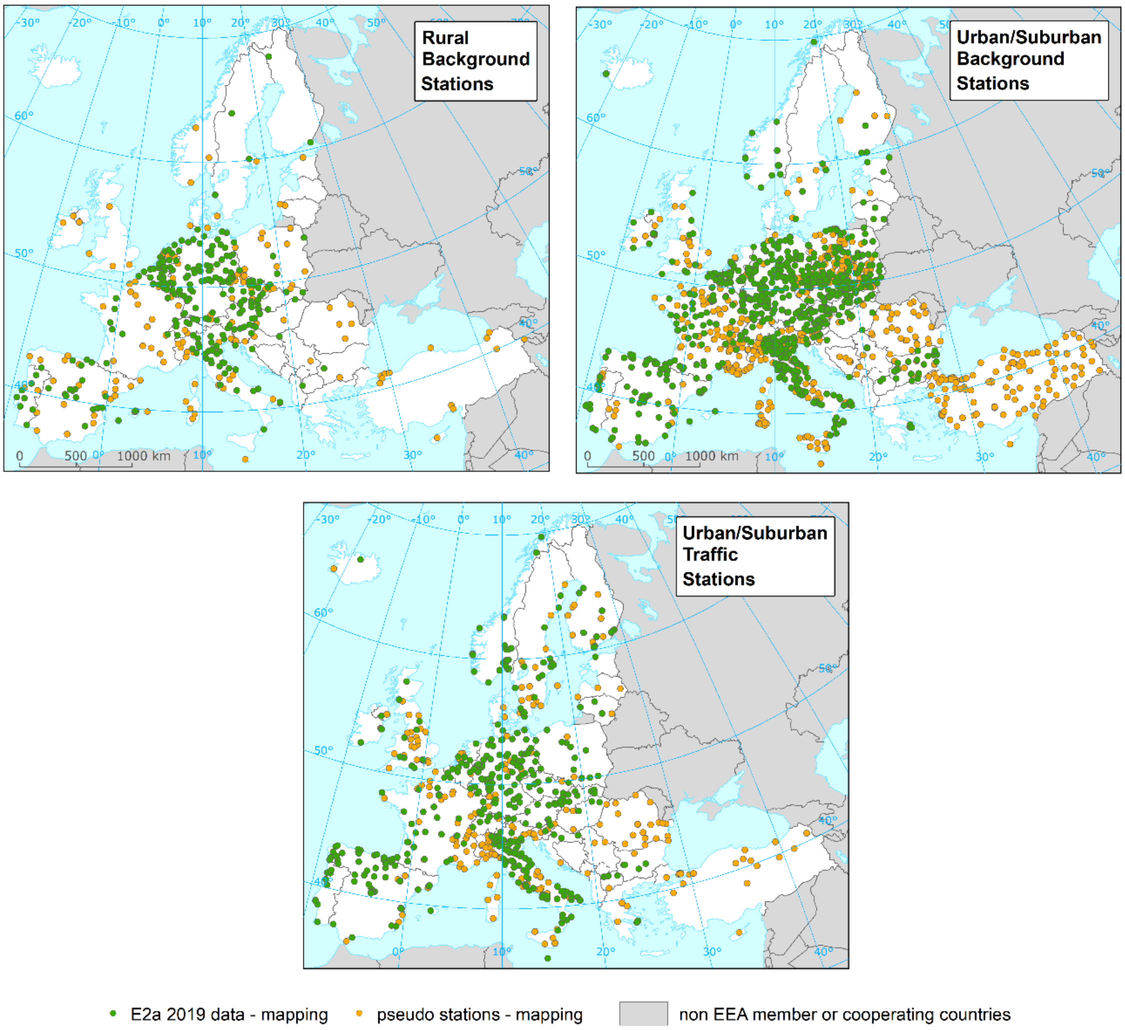

Map A.5 Spatial distribution of NO_2 stations used in interim mapping, 2019

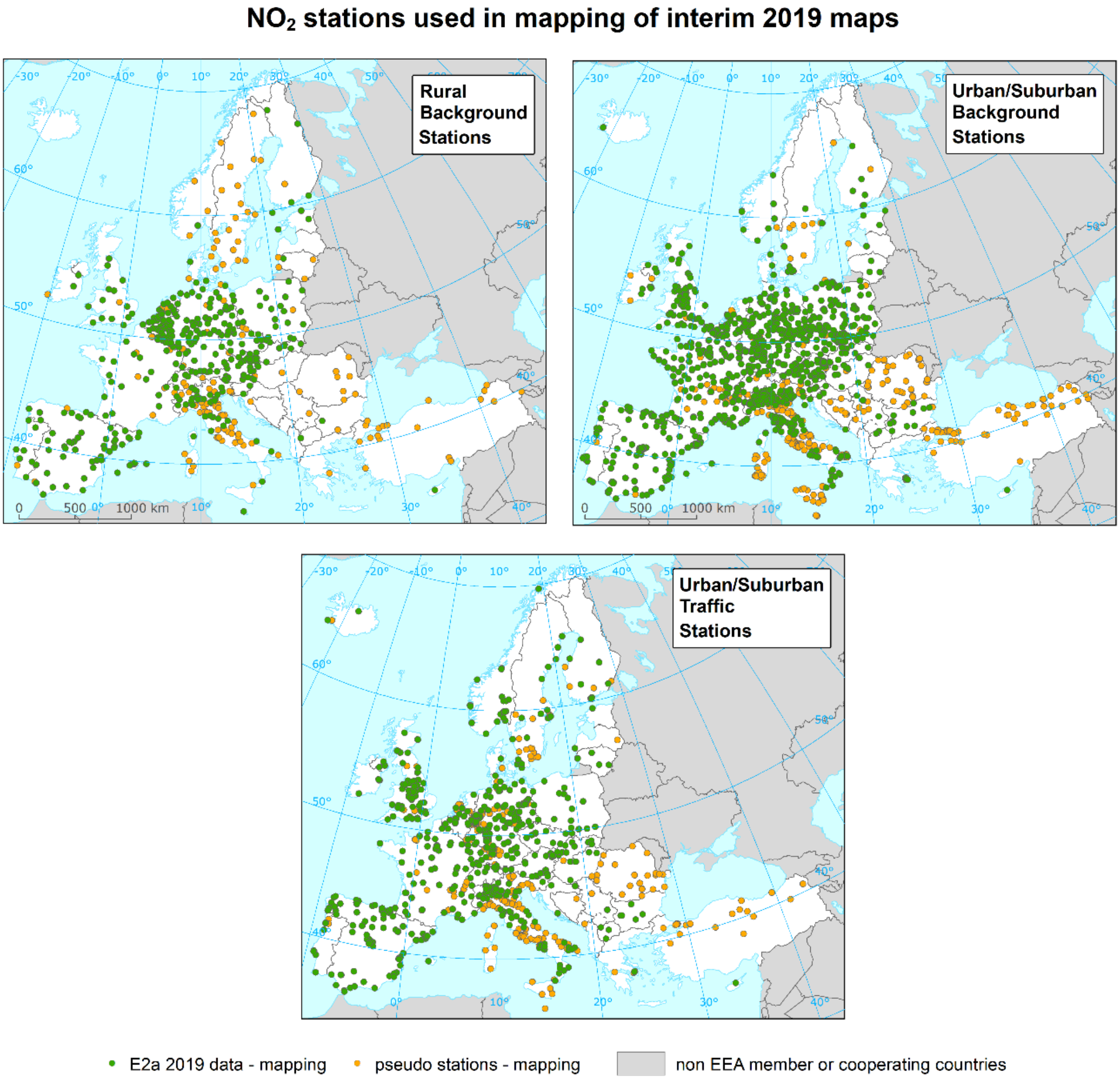

Map A.6 Spatial distribution of O_3 background stations used in interim mapping, 2019

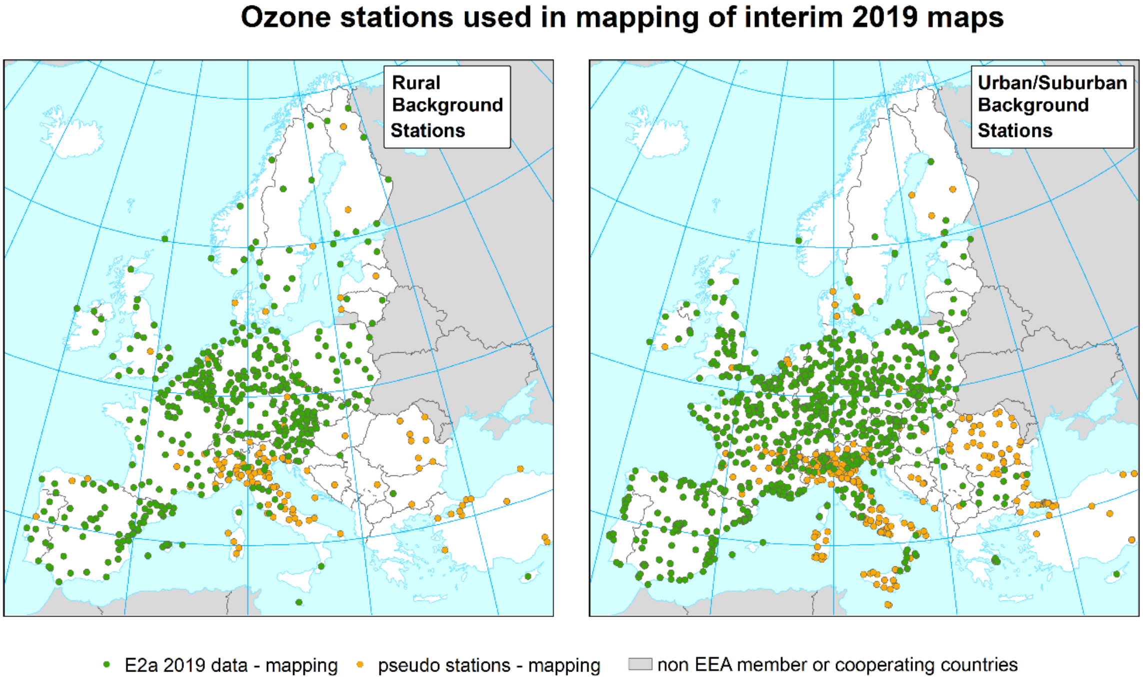

European Topic Centre on Air pollution,
transport, noise and industrial pollution
c/o NILU – Norwegian Institute for Air Research
P.O. Box 100, NO-2027 Kjeller, Norway
Tel.: +47 63 89 80 00
Email: etc.atni@nilu.no
Web : https://www.eionet.europa.eu/etcs/etc-atni

The European Topic Centre on Air pollution, transport, noise and industrial pollution (ETC/ATNI) is a consortium of European institutes under a framework partnership contract to the European Environment Agency.

European Environment Agency
European Topic Centre on Air pollution,
transport, noise and industrial pollution